only the extensive expression of α-SG in Sgca$^{-/-}$ skeletal muscle, but also a robust level of expression of α-SG at the sarcolemma after a single intramuscular injection of rAAV8-α-SG. In addition, rAAV8-α-SG effectively transduced the cardiac muscle of 7-week-old Sgca$^{-/-}$ mice (adult Sgca$^{-/-}$ mice). Most importantly, 7 months after the injection of rAAV8-α-SG into neonatal Sgca$^{-/-}$ mice, expression of α-SG and improvement of sarcolemmal function were sustained, without inducing cytotoxic and immunological reactions. Thus, the AAV8 vector is a promising tool for gene therapy of LGMD 2D.

Materials and Methods

Recombinant AAV production

The full-length human α-SG cDNA was amplified from a skeletal muscle single-strand cDNA library (Human Skeletal Muscle Marathon-Ready cDNA; Clontech, Palo Alto, CA) by polymerase chain reaction (PCR) with the following set of oligonucleotide primers: 5′-CTCTGTCACTCACCGGG-3′ (nucleotide positions 2–18) and 5′-AGGATGAAGTC-AGGGCTGGAC-3′ (nucleotide positions 1223–1243) (McNally *et al.*, 1994). The amplification was carried out with LA-Taq polymerase (TaKaRa Bio, Shiga, Japan) for 30 cycles, with each cycle consisting of 94°C for 30 sec and 60°C for 2 min. The PCR products were then cloned into a TA cloning vector (Invitrogen, Carlsbad, CA), and sequenced with an ABI310 sequencer (Applied Biosystems, Foster City, CA). α-SG cDNA was then cloned into an AAV serotype 2 vector plasmid (Xiao *et al.*, 1998; Yuasa *et al.*, 2002) including the cytomegalovirus (CMV) promoter, splicing donor/acceptor (SD/SA) sites derived from the simian virus 40 (SV40), an SV40 poly(A) signal, inverted terminal repeat (ITR) of the AAV2 viral genome, and 2.0 kb of λ DNA, which served as a stuffer (depicted in Fig. 1A).

The vector genome was packaged in the AAV2 capsid or pseudotyped into the AAV8 capsid by triple transfection of

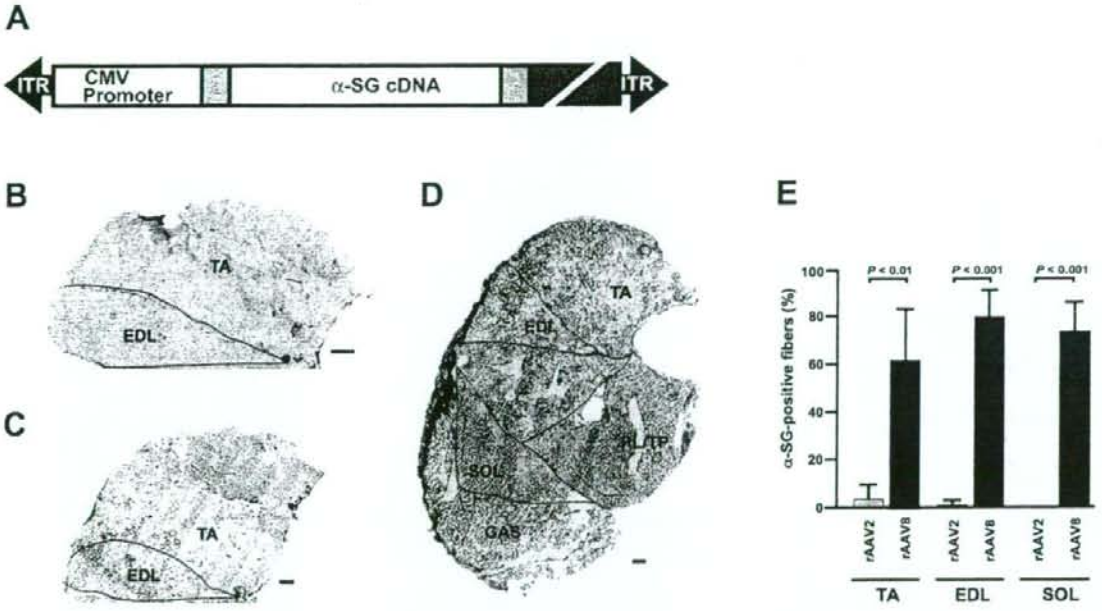

FIG. 1. Widespread expression of α-SG in hind limb muscles after a single injection of rAAV2-α-SG or rAAV8-α-SG into the tibialis anterior (TA) muscles of 10-day-old α-SG-deficient mice. (**A**) Genomic structure of rAAV used in this study. Human α-SG cDNA (1.2 kb) was inserted downstream of the CMV promoter. ITR, inverted terminal repeat from AAV2 genome; SD/SA, splicing donor/acceptor sites derived from SV40 intron; poly(A), a polyadenylation signal from SV40. The large shaded box represents a stuffer sequence derived from λ DNA. (**B–D**) Right TA muscles of neonatal Sgca$^{-/-}$ mice were injected with 1×10^{11} VG of rAAV2-α-SG (**C**) or rAAV8-α-SG (**D**). Four weeks after rAAV injection, the hind limb muscles of Sgca$^{-/-}$ mice were immunolabeled with a rabbit polyclonal antibody to α-SG. Hind limb muscles included the TA, extensor digitorum longus (EDL), plantaris (PL)/tibialis posterior (TP), soleus (SOL), and gastrocnemius (GAS) muscles. The TA and EDL muscles of Sgca$^{-/-}$ mice are shown as negative controls (**B**). Note that α-SG is expressed not only in rAAV8-injected TA muscle, but also in all hind limb muscles after direct injection of rAAV8-α-SG into the right TA muscle (**D**). Scale bars (**B–D**): 500 μm. (**E**) Percentages of α-SG-positive myofibers in TA, EDL, and SOL muscles after injection of rAAV2-α-SG (shaded columns) and rAAV8-α-SG (solid columns) injection into TA muscles of Sgca$^{-/-}$ mice. The right TA muscles of neonatal Sgca$^{-/-}$ mice were transduced with 1×10^{11} VG of rAAV2-α-SG or rAAV8-α-SG. Four weeks after rAAV injection, the hind limb muscles of Sgca$^{-/-}$ mice were immunolabeled with the α-SG antibody and then counterstained with hematoxylin and eosin. Hind limb muscles include the TA, EDL, and SOL muscles. The percentage of α-SG-positive myofibers was calculated on the basis of more than 200 total myofibers in cross-sections from three animals for each group. *p* Values are indicated and show statistical significance between Sgca$^{-/-}$ mice and rAAV8-injected Sgca$^{-/-}$ mice ($p < 0.01$ for TA, $p < 0.001$ for EDL, and $p < 0.001$ for SOL).

the AAV vector plasmid, AAV helper plasmid (p5E18-VD2/8) (Wang *et al.*, 2005), and adenovirus helper plasmid (XX6) (Xiao *et al.*, 1998) at a molecular ratio of 1:1:1 in 293 cells, using the calcium phosphate coprecipitation method (Wigler *et al.*, 1980). All the vectors were then purified by two cycles of cesium chloride gradient centrifugation, and concentrated as described by Burton and coworkers (1999). The final viral preparations were kept in phosphate-buffered saline. Physical particle titers were determined by a quantitative dot-blot assay.

Administration of rAAV vectors to murine skeletal muscle

All animal-handling procedures were done in accordance with a protocol approved by the committee of the National Institute of Neuroscience (National Center of Neurology and Psychiatry, Kodaira, Japan). Wild-type ($Sgca^{+/+}$) and $Sgca^{-/-}$ mice (Burnham Institute, La Jolla, CA) were used. The TA muscles of 10-day-old (neonate) and 7-week-old (adult) $Sgca^{-/-}$ mice were transduced with 1×10^{11} vector genomes (VG) (10 μl) and 5×10^{11} VG (50 μl), respectively, of rAAV2- or rAAV8-α-SG, using 29-gauge needles.

Transgene expression analyses

Histological and immunohistochemical analyses were performed as described (Imamura *et al.*, 2000; Yuasa *et al.*, 2002). Cryosections (6 μm thick) were prepared from frozen muscle.

For colorimetric immunodetection of α-SG, blocked cryosections were incubated with a 1:1000 dilution of rabbit polyclonal anti-α-SG (Araishi *et al.*, 1999) for 1 hr at room temperature. The signal was visualized with a VECTASTAIN ABC kit (Vector Laboratories, Burlingame, CA) and then counterstained with hematoxylin and eosin (H&E). Stained sections were photographed with a light microscope (Leica, Heidelberg, Germany) using DP70 image scanning software (Olympus, Tokyo, Japan).

For fluorescence immunohistochemical detection of SGs, cryosections were fixed by immersion in cold acetone at −20°C for 5 min. After blocking with 2% casein in Tris-buffered saline (TBS, pH 7.4) at room temperature for 1 hr, α-SG was detected with rabbit polyclonal anti-α-SG (1:1000 dilution) (Araishi *et al.*, 1999). β-, γ-, and δ-SGs were detected with mouse monoclonal anti-β-SG (NCL-b-SARC, 1:50 dilution; Novocastra Laboratories, Newcastle-upon-Tyne, UK), anti-γ-SG (1:50 dilution), and anti-δ-SG (DSG-1; 1:50 dilution), respectively, after blocking with an M.O.M. kit (Vector Laboratories). Mouse monoclonal antibodies against γ-SG and δ-SG (DSG-1) were generated in our laboratory (Yamamoto *et al.*, 1994; Noguchi *et al.*, 1999). The signal was visualized with Alexa 488-conjugated anti-rabbit and anti-mouse IgG antibodies (Invitrogen Molecular Probes, Eugene, OR). Fluorescence signals were observed with a confocal laser-scanning microscope (Leica TCS SP; Leica).

Sodium dodecyl sulfate–polyacrylamide gel electrophoresis (SDS–PAGE) and protein transfer to a polyvinylidene di-

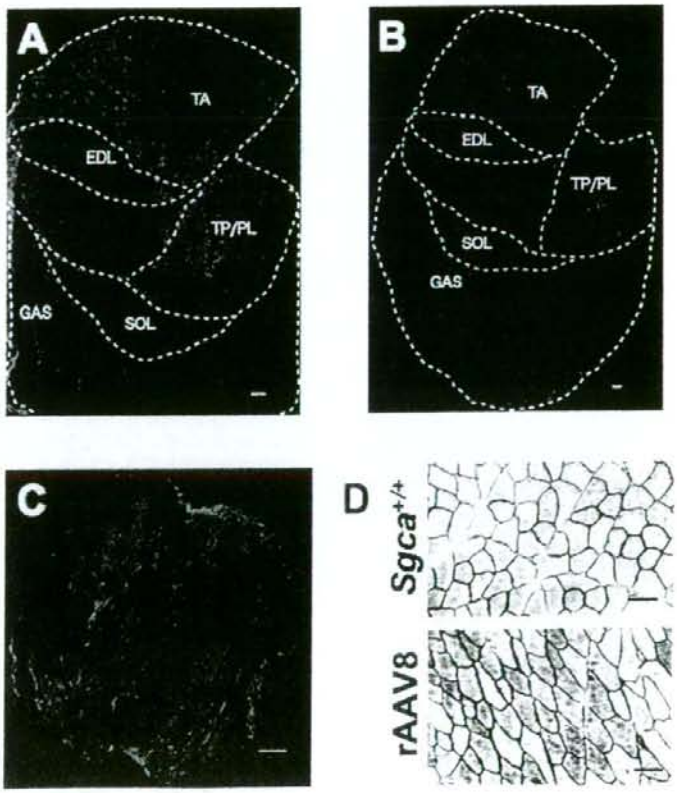

FIG. 2. Extensive α-SG expression after injection of rAAV8-α-SG into TA muscles of 7-week-old α-SG-deficient mice. Right TA muscles of adult $Sgca^{-/-}$ or $Sgca^{+/+}$ mice were transduced with 5×10^{11} VG of rAAV8-α-SG. Four weeks after rAAV8 injection, a cross-section of the right hind limb muscles (rAAV8-injected) (**A**), left contralateral hind limb muscles (**B**), and cardiac apex (**C**) were labeled by indirect immunofluorescence, using α-SG antibody (green). Scale bars: (**A** and **B**) 500 μm; (**C**) 100 μm. Note the widespread expression of α-SG in the hind limb muscles and cardiac muscle of rAAV8-α-SG-injected mice. (**D**) Cross-sections of TA muscle from $Sgca^{+/+}$ and rAAV8-injected $Sgca^{+/+}$ (rAAV8) mice were immunolabeled with α-SG antibody and counterstained with hematoxylin and eosin. Overexpression of α-SG caused no cytotoxic reactions in $Sgca^{+/+}$ muscle. Scale bars (**D**): 50 μm.

fluoride (PVDF) membrane were performed as described by Laemmli (1970) and Kyhse-Andersen (1984), respectively. Protein concentrations were determined with a protein assay kit (Bio-Rad, Hercules, CA) with bovine serum albumin as a standard.

Transgene copy number analyses

Cryosections of mouse hind limb muscle were collected for vector copy number analysis by quantitative PCR. After DNA extraction by successive treatments with RNase and proteinase K, viral genomes were quantified by a real-time PCR assay using SYBR *Premix Ex Taq* (TaKaRa Bio). The real-time PCR was carried out for 40 cycles, with each cycle consisting of 95°C for 5 sec, 60°C for 10 sec, 72°C for 10 sec, and 75°C for 10 sec. Oligonucleotide primers for this assay were 5'-CTCTAGAGGATCCGGTACTCGAGGAAC-3' (SD/SA sites) and 5'-AGAGGAGTCCAGAAGAGTGTCTCAGCC-3' (human α-SG gene) for the α-SG gene in the rAAV2 genome and 5'-TGCCATGAGCAGCCCATTTTG-3' and 5'-ATAACATCGCGGTGGCTCAGG-3' for the slug promoter. The slug promoter was used for normalization of data across samples.

Analysis of toxicity

Blood was obtained from a murine heart. Serum alanine aminotransferase, γ-glutamyl transpeptidase, albumin, and total protein concentration were determined with a Fuji Dri-Chem slide system (Fujifilm, Tokyo, Japan).

Muscle physiological function

TA and extensor digitorum longus (EDL) muscles were exposed by removal of overlying connective tissue (Xiao *et al.*, 2000; Yoshimura *et al.*, 2004; Imamura *et al.*, 2005). Both tendons of the TA and EDL muscles were cut from their insertions and secured with 5-0 silk sutures. Muscles were mounted in a vertical tissue chamber containing physiological salt solution (150 m*M* NaCl, 4 m*M* KCl, 1.8 m*M* $CaCl_2$, 1 m*M* $MgCl_2$, 5 m*M* HEPES, 5.6 m*M* glucose [pH 7.4], and 0.02 m*M* D-tubocurarine) maintained at 37°C with continuous aeration. The chamber was connected to a force transducer (UL-10GR; Minerva, Nagano, Japan) and a length servosystem (MM-3; Narishige, Tokyo, Japan). Electrical stimulation (SEN3301; Nihon Kohden, Tokyo, Japan) was delivered through a pair of platinum wires placed on both sides of the muscle. The muscle fiber length was adjusted incrementally with a micropositioner until peak isometric twitch force responses were obtained (i.e., optimal fiber length L_o). L_o was measured with a microcaliper. Maximal tetanic force (P_o) was induced by stimulation frequencies of 125 pulses per second, delivered in trains of 500-msec duration with 2-min intervals between each train. The muscle was weighed, rapidly frozen in liquid nitrogen-cooled isopentane, and stored at –80°C for further analysis. All forces were normalized to the physiological cross-section area (CSA), which was estimated on the basis of the following formula: muscle wet weight (in mg)/[L_o (in mm) × 1.06 (in mg/mm^3)]. The estimated CSA was used to determine specific tetanic (P_o/CSA) force of the muscle. Data are presented as means ± SE. Differences between groups were assessed by Student *t* test.

Exercise tolerance tests

Mice were subjected to an exhaustion treadmill test (Mourkioti *et al.*, 2006). Each mouse was placed on the belt of a four-lane motorized treadmill (MK-680; Muromachi Kikai, Tokyo, Japan) supplied with shocker plates. The treadmill was run at an inclination of 7 degrees at 5 m/min for 5 min, after which the speed was increased by 1 m/min every minute. The test was terminated when the mouse remained on the shocker plate for more than 20 sec without attempting to reengage the treadmill, and the time to exhaustion was determined.

Results

Expression of α-SG after injection of rAAV2- or rAAV8-α-SG into TA muscles of neonatal α-SG-deficient mice

We constructed rAAV2- and rAAV8-α-SG expressing human α-SG cDNA under the control of the ubiquitous CMV promoter, and injected 1×10^{11} VG into the right TA muscle of neonatal Sgca$^{-/-}$ mice (Fig. 1A). Neonatal Sgca$^{-/-}$ mice showed no obvious dystrophic changes, whereas adult (>4 weeks old) Sgca$^{-/-}$ skeletal muscles showed active cycles of the degeneration–regeneration process. In the hind limb muscles of 5-week-old Sgca$^{-/-}$ mice, α-SG-positive

TABLE 1. EFFECT OF rAAV2- AND rAAV8-α-SARCOGLYCAN ADMINISTRATION ON THE LIVER FUNCTION OF ADULT Sgca$^{-/-}$ MICE 4 WEEKS AFTER INJECTION[a,b]

	Number of mice	*ALT (U/liter)*	*γ-GTP (U/liter)*	*ALB (g/dl)*	*TP (g/dl)*
Sgca$^{+/+}$	3	26.67 ± 8.50[c]	<10	2.43 ± 0.21	4.80 ± 0.20
Sgca$^{-/-}$	3	145.33 ± 22.22	<10	2.33 ± 0.23	4.60 ± 0.42
rAAV2-injected Sgca$^{-/-}$	3	149 ± 9[d]	<10	2.10 ± 0.44	4.00 ± 0.53
rAAV8-injected Sgca$^{-/-}$	3	124 ± 15.10[e]	<10	2.03 ± 0.25	4.60 ± 0.89

Abbreviations: ALT/GPT, alanine aminotransferase/glutamic pyruvic transaminase; γ-GTP, γ-glutamyl transpeptidase; ALB, albumin; TP, total protein.

[a]Data represent means ± SE.

[b]The *p* values indicate statistical significance. Significant differences from the ALT/GPT level of Sgca$^{-/-}$ mice are indicated.

[c]$p < 0.001$.

[d]$p = 0.797$.

[e]$p = 0.229$.

fibers were not observed and the active cycle of muscle degeneration–regeneration was present (Fig. 1B). Four weeks after a single intramuscular injection of rAAV2-α-SG, α-SG was expressed only in a limited area of rAAV2-injected TA muscle (Fig. 1C and E). Analysis of TA muscle showed that less than 10% of muscle fibers were α-SG positive ($p < 0.01$; Fig. 1E).

In contrast, after rAAV8-α-SG injection, α-SG-positive fibers were widely spread in rAAV8-injected hind limb muscles, including the TA, extensor digitorum longus (EDL), soleus (SOL), gastrocnemius (GAS), and plantaris (PL)/tibialis posterior (TP) muscles (Fig. 1D). Analysis of the TA, EDL, and SOL muscles showed 62.3 ± 20.2, 79.5 ± 11.0, and 74.2 ± 11.2% α-SG-positive fibers, respectively ($p < 0.01$, $p < 0.001$, and $p < 0.001$; Fig. 1E). The expression of α-SG in rAAV8-α-SG-injected TA muscle and surrounding muscles persisted more than 7 months (data not shown).

Expression of α-SG after injection of rAAV2-α-SG or rAAV8-α-SG into TA muscles of adult α-SG-deficient mice

Adult Sgca$^{-/-}$ mice (>4 weeks old) showed active cycles of the degeneration–regeneration process and had a mature immune system. To investigate whether injection of rAAV2-α-SG or rAAV8-α-SG could induce stable expression of α-SG in adult Sgca$^{-/-}$ skeletal muscle without cytotoxicity and immune response, we injected 5×10^{11} VG of rAAV2-α-SG or rAAV8-α-SG into the right TA muscles of adult Sgca$^{-/-}$ mice. Four weeks after rAAV2-α-SG injection, we did not observe α-SG-positive fibers in the right TA muscle (data not shown). rAAV2-α-SG-injected TA muscles showed the degeneration–regeneration process. In contrast, after rAAV8-α-SG injection, we observed numerous α-SG-positive fibers in the entirety of rAAV8-injected hind limb muscles (Fig. 2A). Moreover, α-SG-positive fibers were detected even in contralateral hind limb muscles and cardiac muscle (Fig. 2B and C). In particular, when rAAV8-α-SG was injected into the TA muscle of Sgca$^{+/+}$ mice, we observed no pathological changes in the injected hind limb muscles 4 weeks after injection (Fig. 2D). No signs of tissue damage were found in regions where α-SG was detected after injection of rAAV8-α-SG. α-SG-positive myofibers retained normal morphology up to 4 weeks after injection. In addition, to examine whether rAAV2-α-SG and rAAV8-α-SG administration affect liver function, we measured the serum level of liver-related isozymes including alanine aminotransferase (ALT), γ-glu-

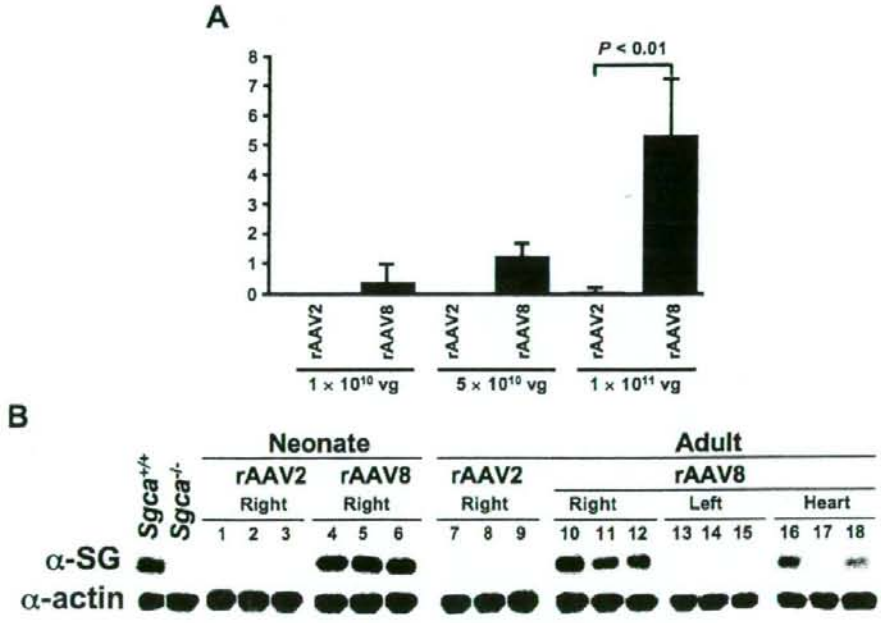

FIG. 3. Immunoblot analysis of α-SG in rAAV-injected α-SG-deficient muscles. Expression of α-SG in the hind limb muscles and heart of Sgca$^{-/-}$ mice was examined 4 weeks after rAAV injection, by real-time PCR and Western blot. (**A**) Real-time PCR was performed in duplicate to quantitate transgene copy number in each hind limb muscle after a single intramuscular administration of rAAV2-α-SG and rAAV8-α-SG. The right TA muscle of neonatal Sgca$^{-/-}$ mice was transduced with vector at 1×10^{10}, 5×10^{10}, and 1×10^{11} VG. Results are represented as vector copy number per diploid genome together with standard errors of mean. p Values are indicated and show a significant difference between rAAV2- and rAAV8-injected Sgca$^{-/-}$ mice ($p < 0.001$). (**B**) The right TA muscles of Sgca$^{-/-}$ mice were transduced with 1×10^{11} VG (neonates) or 5×10^{11} VG (adults) of rAAV2-α-SG (lanes 1–3 and 7–9) or rAAV8-α-SG (lanes 4–6 and 10–18). Ten-microgram samples of muscle lysates were separated by 10% SDS–PAGE. Faint bands were detected in the contralateral hind limb muscles of rAAV8-α-SG-injected mice. Adult Sgca$^{+/+}$ and Sgca$^{-/-}$ hind limb muscle lysates were used as positive and negative controls, respectively. The α-SG antibody detected a 50-kDa band. α-Sarcomeric actin is shown as a loading control.

tamyl transpeptidase (γ-GTP), albumin (ALB), and total protein (TP) in rAAV2-α-SG- and rAAV8-α-SG-injected Sgca$^{-/-}$ mice. Because skeletal muscle contains isozymes of creatine kinase, lactate dehydrogenase, aspartate aminotransferase, and ALT, these may be released into the blood stream after muscle necrosis (Janssen *et al.*, 1989); the ALT level in Sgca$^{-/-}$ mice was 5.4-fold higher than that in Sgca$^{+/+}$ mice ($p < 0.001$; Table 1). The ALT level in rAAV8-injected Sgca$^{-/-}$ mice was slightly lower than that in Sgca$^{-/-}$ mice. The levels of other liver-related proteins, including γ-GTP, ALB, and TP, were not significantly different between Sgca$^{-/-}$ and rAAV2-α-SG- and rAAV8-α-SG-injected Sgca$^{-/-}$ mice.

Tropism of rAAV2- and rAAV8-α-SG in α-SG-deficient mice

To investigate whether there is any difference in tissue tropism between rAAV2 and rAAV8, we determined the vector copies per diploid genome (C/DG) between the two vectors in injected skeletal muscle by a quantitative, real-time PCR assay. We injected neonatal Sgca$^{-/-}$ mice with either rAAV2-α-SG or rAAV8-α-SG at three different doses (1×10^{10}, 5×10^{10}, or 1×10^{11} VG/mouse) via the TA muscle ($n = 3$ per group). At a dose of 1×10^{11} VG/mouse, we detected rAAV2-α-SG and rAAV8-α-SG vector genomes in skeletal muscle at levels of 0.05 ± 0.03 and 5.33 ± 1.88 C/DG, respectively ($p < 0.01$; Fig. 3A). Increasing doses of rAAV8-α-SG resulted in increased levels of transgene expression. Higher transduction efficiency was observed with rAAV8-α-SG when large amounts of vector were used. Moreover, to evaluate the amount of α-SG in rAAV2-α-SG- or rAAV8-α-SG-injected skeletal muscles of Sgca$^{-/-}$ mice, we performed Western blot analysis. Four weeks after injection of rAAV2-α-SG into the TA muscle of neonatal and adult Sgca$^{-/-}$ mice, α-SG was almost undetectable (Fig. 3B). In contrast, when rAAV8-α-SG was injected into the right TA muscle of neonatal Sgca$^{-/-}$ mice, the amount of α-SG in rAAV8-transduced muscles was 3.5-fold higher than that in Sgca$^{+/+}$ muscles. When transduced in adulthood, the expression level of α-SG in the TA muscle of Sgca$^{-/-}$ mice was almost equal to that in Sgca$^{+/+}$ muscle. In addition, α-SG was detected in contralateral hind limb muscles and the heart after injection of rAAV8-α-SG into the TA muscle (Fig. 3B).

rAAV8-mediated α-SG expression ameliorated muscle pathology

A defect in any one of the four SGs can disrupt the entire SG complex in LGMD 2C-2F patients. Thus, we investigated the presence of a SG complex in the sarcolemma 4 weeks after injection of rAAV8-α-SG into the TA muscle of neonatal Sgca$^{-/-}$ mice. Immunostaining of rAAV8-α-SG-injected TA muscle with anti-SGs antibodies revealed that restoration of α-SG expression accompanied the sarcolemmal expression of other components of the SG complex, that is, β-, γ-, and δ-SG (Fig. 4). Moreover, 4 weeks after rAAV8-α-SG injection, H&E staining demonstrated considerable amelioration of the muscle pathology of rAAV8-injected TA muscles (Fig. 5A), and of surrounding EDL, SOL, GAS, and TP/PL muscles (data not shown). In contrast, uninjected and rAAV2-α-SG-injected muscles of Sgca$^{-/-}$ mice still showed signs of muscle degeneration and regeneration. To evaluate the amelioration of the dystrophic phenotype (Morgan *et al.*, 1990; Duclos *et al.*, 1998; Li *et al.*, 1999; Allamand *et al.*, 2000; Dressman *et al.*, 2002), we counted centrally nucleated myofibers in rAAV8-α-SG-injected muscles 4 months after injection (Fig. 5B). Sgca$^{-/-}$ hind limb muscles showed approximately 90% centrally nucleated myofibers. In contrast, rAAV8-α-SG-injected TA and ipsilateral EDL and SOL muscles showed

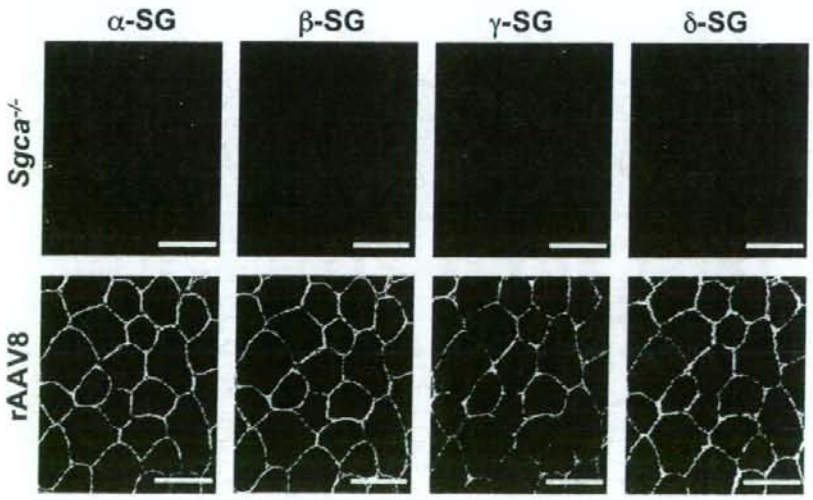

FIG. 4. Complete restoration of sarcoglycan expression at the sarcolemma of α-SG-deficient muscle after rAAV8-α-SG injection. Right TA muscles of neonatal Sgca$^{-/-}$ mice were injected with 1×10^{11} VG of rAAV8-α-SG. Untreated and rAAV8-injected Sgca$^{-/-}$ TA muscles (*top* and *bottom*, respectively) were labeled by indirect immunofluorescence, using specific antibodies against β-SG, γ-SG, or δ-SG. Untreated Sgca$^{-/-}$ muscle showed a secondary loss of SGs from the sarcolemma. Four weeks after injection, SGs were expressed in rAAV8-injected Sgca$^{-/-}$ muscle. Scale bars: 50 μm.

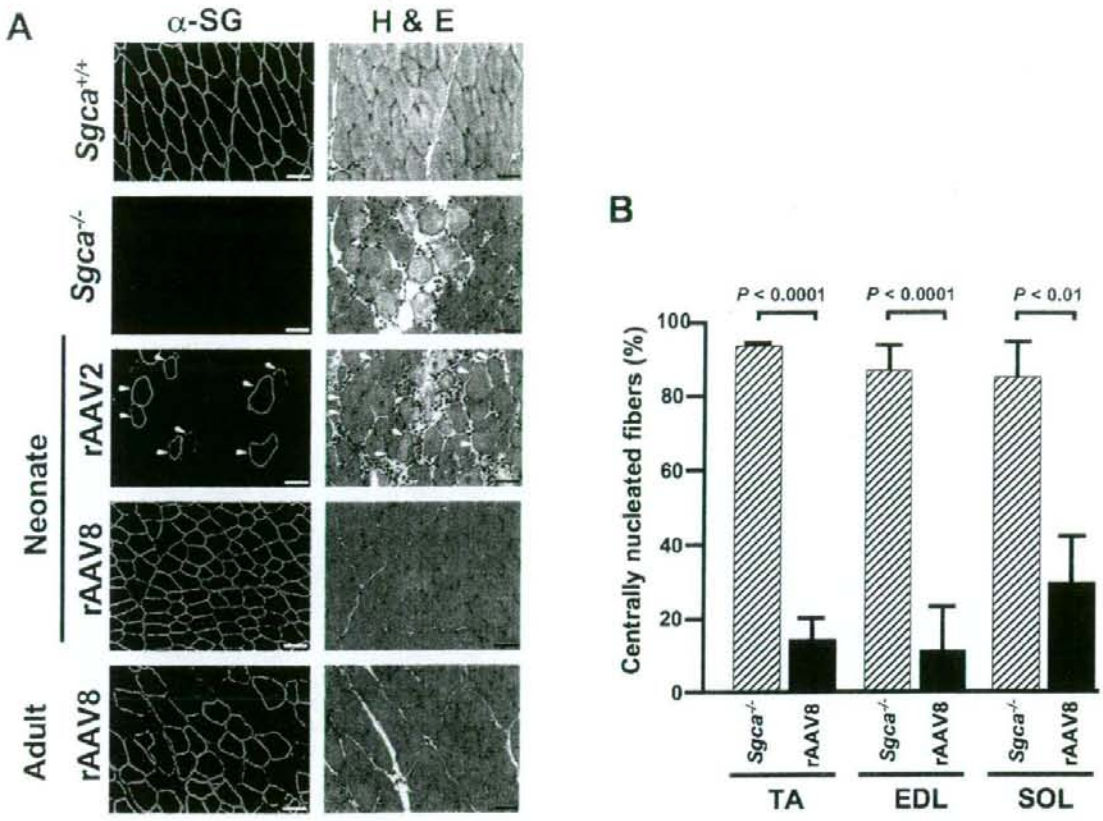

FIG. 5. Reduction of muscle degeneration in α-SG-deficient mice after rAAV8-α-SG-mediated gene transfer. (**A**) Right TA muscles of neonatal or adult Sgca$^{-/-}$ mice were transduced with 1×10^{11} VG (neonates) or 5×10^{11} VG (adults) of rAAV2-α-SG or rAAV8-α-SG. Four weeks after rAAV injection, serial cross-sections of Sgca$^{+/+}$, Sgca$^{-/-}$, and rAAV2- or rAAV8-injected Sgca$^{-/-}$ TA muscles (rAAV2 and rAAV8, respectively) were labeled by indirect immunofluorescence, using α-SG antibody (*left*, green), and stained with hematoxylin and eosin (H&E) (*right*). rAAV8-injected Sgca$^{-/-}$ TA muscles showed no signs of muscle degeneration. Arrowheads indicate α-SG-positive fibers. Scale bars: 50 μm. (**B**) Percentages of centrally nucleated myofibers in Sgca$^{-/-}$ skeletal muscles 4 months after injection of rAAV8-α-SG. Right TA muscles of neonatal Sgca$^{-/-}$ mice were transduced with 1×10^{11} VG of rAAV8-α-SG. Centrally nucleated myofibers among more than 200 total myofibers were counted in randomly selected H&E-stained cross-sections of the hind limb from Sgca$^{-/-}$ mice (hatched columns) and rAAV8-α-SG-injected Sgca$^{-/-}$ mice (solid columns) ($n = 3$ for each group). The percentage of centrally nucleated myofibers in rAAV8-α-SG-injected Sgca$^{-/-}$ mice was significantly lower than that in untreated Sgca$^{-/-}$ mice. p Values showed a statistically significant difference between Sgca$^{-/-}$ mice and rAAV8-injected Sgca$^{-/-}$ mice ($p < 0.0001$ for TA, $p < 0.0001$ for EDL, and $p < 0.01$ for SOL).

13.2 ± 7.3, 10.4 ± 10.4, and 29.1 ± 12.9% centrally nucleated myofibers, respectively ($p < 0.0001$, $p < 0.0001$, and $p < 0.0023$, respectively; Fig. 5B). The percentage of centrally nucleated myofibers in rAAV8-injected hind limb was significantly lower than that of Sgca$^{-/-}$ muscle, indicating that full recovery of the SG complex at the sarcolemma of Sgca$^{-/-}$ mice corrected the underlying biochemical deficiency and consequently restored the integrity of the muscle membrane.

rAAV-8-mediated α-SG expression improves contractile force and reverses muscle hypertrophy of α-SG-deficient muscle

A major functional deficit in muscular dystrophy patients is the loss of muscle strength. In our previous physiological study of muscular dystrophy model animals, we confirmed profound muscle force deficits in TA muscle (Yoshimura *et al.*, 2004; Imamura *et al.*, 2005).

A deficiency of α-SG decreases the contractile force of affected muscles (Danieli-Betto *et al.*, 2005; Imamura *et al.*, 2005). To evaluate whether rAAV8-α-SG transfer might improve Sgca$^{-/-}$ muscle physiological function, we measured the contractile force of rAAV8-injected Sgca$^{-/-}$ TA and EDL muscles. TA and EDL muscles were carefully separated from the hind limb and subjected to *in vitro* electrophysiological stimulation and contractile measurement on a force transducer. First, the right TA muscles of neonatal Sgca$^{-/-}$ mice were transduced with 1×10^{11} VG of rAAV8-α-SG. At the age of 5 months, the specific tetanic force of untreated Sgca$^{+/+}$ and Sgca$^{-/-}$ TA muscles was 17.3 ± 4.5 and 8.9 ±

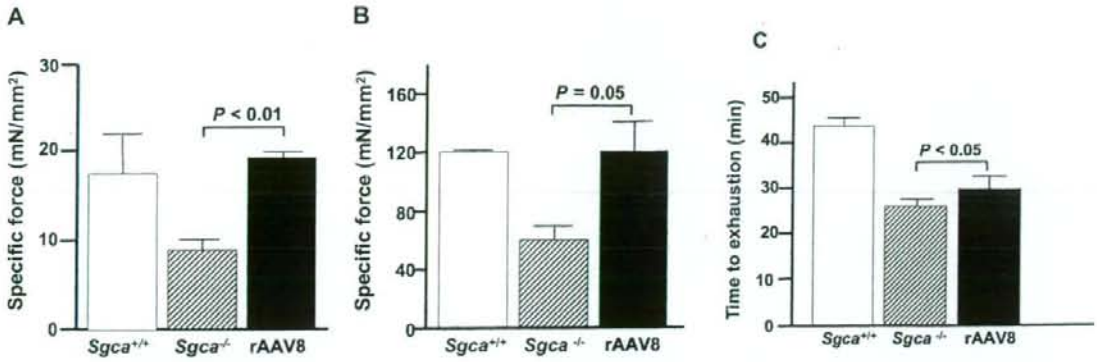

FIG. 6. Recovery of contractile force of α-SG-deficient muscle after transduction with rAAV8-α-SG. Right TA muscles of neonatal or adult Sgca$^{-/-}$ mice were transduced with 1×10^{11} VG (neonates) or 5×10^{11} VG (adults) of rAAV8-α-SG, and tetanic forces and time to exhaustion were assessed *in vitro* and *in vivo*. (**A**) Specific tetanic force of TA muscles from Sgca$^{+/+}$ (open column, $n = 3$), untreated Sgca$^{-/-}$ (hatched column, $n = 3$), and rAAV8-α-SG-injected Sgca$^{-/-}$ mice (solid column, $n = 3$). The right TA muscles of neonatal Sgca$^{-/-}$ mice were transduced with 1×10^{11} VG of rAAV8-α-SG, and the tetanic forces of TA muscles were assessed *in vitro* 5 months after injection. (**B**) Specific tetanic force of EDL muscles from Sgca$^{+/+}$ (open column, $n = 3$), untreated Sgca$^{-/-}$ (hatched column, $n = 3$), and rAAV8-α-SG-injected Sgca$^{-/-}$ mice (solid column, $n = 4$). The right TA muscles of adult Sgca$^{-/-}$ mice were transduced with 5×10^{11} VG of rAAV8-α-SG, and the tetanic forces of EDL muscles were assessed *in vitro* 10 weeks after injection. The p values show a statistically significant difference between Sgca$^{-/-}$ mice and rAAV8-injected Sgca$^{-/-}$ mice ($p < 0.01$ for TA, and $p = 0.05$ for EDL). (**C**) Time to exhaustion in treadmill test: Sgca$^{+/+}$ (open column, $n = 3$), untreated Sgca$^{-/-}$ (hatched column, $n = 4$), and rAAV8-α-SG-injected Sgca$^{-/-}$ mice (solid column, $n = 4$). The right TA muscles of adult Sgca$^{-/-}$ mice were transduced with 5×10^{11} VG of rAAV8-α-SG, and the tetanic forces of EDL muscles were assessed *in vitro* 10 weeks after injection. The p values show a statistically significant difference between Sgca$^{-/-}$ mice and rAAV8-injected Sgca$^{-/-}$ mice ($p < 0.05$).

1.2 mN/mm^2, respectively, whereas that of rAAV8-injected Sgca$^{-/-}$ TA muscle was 19.4 ± 0.7 mN/mm^2 ($p < 0.01$; Fig. 6A and Table 2). Furthermore, we assessed the improvement of EDL muscle after rAAV8-α-SG injection in adulthood. rAAV8-α-SG (5×10^{11} VG) was injected into the right TA muscle of adult Sgca$^{-/-}$ mice. We measured the contractile force of the EDL muscle surrounding rAAV8-injected TA muscle 10 weeks after injection. The specific tetanic forces of Sgca$^{+/+}$ and Sgca$^{-/-}$ EDL muscles were 121.5 ± 1.6 and 61.74 ± 8.33 mN/mm^2, and that of rAAV8-injected Sgca$^{-/-}$ EDL muscle was 121.15 ± 22.12 mN/mm^2 ($p = 0.05$; Fig. 6B and Table 2). Consequently, the specific tetanic force of animals injected with rAAV8-α-SG was 2-fold higher than that of uninjected Sgca$^{-/-}$ TA muscle ($p < 0.01$, and $p = 0.05$; Fig. 6A and B, Table 2).

In addition to the drastic improvement in contractile force of rAAV8-α-SG-injected TA muscle, the weight of rAAV8-α-SG-injected TA and EDL muscles as a percentage of body weight was comparable to those of Sgca$^{+/+}$ muscle and much smaller than those of their untreated counterparts (Table 2), suggesting that rAAV8-α-SG treatment reduced the muscle hypertrophy of Sgca$^{-/-}$ muscle. Moreover, we investigated whether α-SG expression in Sgca$^{-/-}$ muscle effectively increases the physical performance of the muscle. In an enforced treadmill test, the exhaustion times of Sgca$^{-/-}$ and rAAV8-α-SG injected Sgca$^{-/-}$ mice were 25.9 ± 2.0 and 30 ± 2.6 min ($p < 0.05$; Fig. 6C). rAAV8-injected Sgca$^{-/-}$ mice demonstrated increased exercise time before reaching exhaustion and could run longer distances.

Discussion

In this paper, we have presented evidence that a single intramuscular injection of a rAAV8 vector expressing human α-SG cDNA via a CMV promoter could achieve efficient therapeutic effects in a dystrophic animal model of LGMD 2D.

When rAAV8-α-SG was administered to neonatal Sgac$^{-/-}$ mice, we observed extensive α-SG transduction in the hind limb muscles, including the TA, EDL, SOL, and GAS muscles. In the case of rAAV8 injection of adult Sgac$^{-/-}$ mice, α-SG was expressed not only in all of the hind limb muscles and but also in cardiac muscle. A similar profile was further confirmed in a study by Wang and coworkers, in which they delivered more potent double-stranded rAAV8 vectors into adult and neonatal mice. The rAAV8 vector is more stable in the bloodstream than other rAAV serotypes when administered intravascularly and extravascularly (Wang *et al.*, 2005). The 37/67-kDa laminin receptor (LamR) has been identified as the host cell receptor for the AAV8 vector (Akache *et al.*, 2006). LamR is widely expressed in human tissues, where it is normally involved in interactions of extracellular laminin-1 with proteases and the cell (Ardini *et al.*, 1997, 2002). Furthermore, the rAAV8 vector might be able to cross the capillary endothelial cell barrier and transduce remote organs with high efficiency (Inagaki *et al.*, 2006). However, the detailed mechanism of rAAV8-mediated cell recognition and transduction has yet to be fully elucidated.

In the present study, we demonstrated that rAAV8-α-SG transduced skeletal muscle about 100-fold more compared with rAAV2-α-SG. In addition, rAAV8-α-SG-injected

TABLE 2. CONTRACTILE PROPERTIES OF rAAV8-INJECTED α-SARCOGLYCAN DEFICIENT MUSCLE[a,b]

	Injection age	*Number of mice*	*Tissue*	*Muscle length* (L_o, *mm*)	*Muscle weight* (*mg*)	*Tissue weight* (*% of body weight*)	*CSA* (mm^2)	*Maximal contraction* (P_o, *mN*)	*Specific force* (mN/mm^2)
$Sgca^{+/+}$	10-day-old	3	TA	11	56.1 ± 2.9	0.185 ± 0.004	4.81 ± 0.14	82.3 ± 19.2	17.3 ± 4.5
$Sgca^{-/-}$	10-day-old	3	TA	11.5	68.1 ± 6.9	0.233 ± 0.023	5.61 ± 0.32	48.5 ± 4.0	8.9 ± 1.2
rAAV8-injected $Sgca^{-/-}$	10-day-old	3	TA	11.5	65.7 ± 8.2	0.224 ± 0.027	5.05 ± 0.46	103.8 ± 10.3	19.4 ± 0.7[c]
$Sgca^{+/+}$	7-week-old	3	EDL	14.83 ± 0.83	11.30 ± 0.46	0.044 ± 0.001	0.73 ± 0.07	88.3 ± 8.5	121.5 ± 1.6
$Sgca^{-/-}$	7-week-old	3	EDL	14	13.5 ± 0.48	0.047 ± 0.002	0.91 ± 0.03	56.94 ± 9.25	61.74 ± 8.33
rAAV8-Injected $Sgca^{-/-}$	7-week-old	4	EDL	14	10.7 ± 0.84	0.038 ± 0.003	0.72 ± 0.06[d]	84.04 ± 8.74	121.15 ± 22.12[e]

Abbreviations: CSA, tissue cross-sectional area; EDL, extensor digitorum longus; TA, tibialis anterior.
[a]Data represent means ± SE. Tissue weights were normalized to respective body weights.
[b]The *p* values indicate statistical significance between $Sgca^{-/-}$ mice and rAAV8-injected $Sgca^{-/-}$ mice.
[c]$p < 0.01$ when rAAV8 was injected into neonatal $Sgca^{-/-}$ TA muscle.
[d]$p \leq 0.05$ when rAAV8 was injected into adult $Sgca^{-/-}$ EDL muscle.
[e]$p \leq 0.05$ when rAAV8 was injected into adult $Sgca^{-/-}$ EDL muscle.

Sgca$^{-/-}$ mice did not demonstrate cytotoxic and immunological reactions for more than 7 months after injection. Transduction of α-SG in an LGMD 2D animal model by means of adenovirus, rAAV1, or rAAV2 vector was previously reported (Duclos *et al.*, 1998; Allamand *et al.*, 2000; Dressman *et al.*, 2002; Fougerousse *et al.*, 2007; Pacak *et al.*, 2007). In the two studies using the adenovirus vector, it was necessary to use neonatal animals to take advantage of the immaturity of the immune system and thereby to circumvent the strong immune response elicited by the adenoviral vector (Duclos *et al.*, 1998; Allamand *et al.*, 2000). The AAV vector, which has been more widely used, is nonpathogenic, has low immunogenicity, and has been shown to confer long-term gene expression in muscles of various species. Use of the ubiquitous CMV promoter would allow expression of the transgene in various cells. Therefore, expression of α-SG via rAAV1 and rAAV2, using the CMV promoter, induced an immune response, whereas those vectors introduced balanced expression of SGs within the injected Sgca$^{-/-}$ myofibers (Duclos *et al.*, 1998; Allamand *et al.*, 2000; Dressman *et al.*, 2002; Fougerousse *et al.*, 2007; Pacak *et al.*, 2007). Between 28 and 41 days after rAAV2 injection, a drastic decrease in α-SG expression occurred in the injected Sgca$^{-/-}$ muscle. In particular, numerous antigen-presenting cells in the dystrophic muscles could direct a strong immune response against the transgene product when the CMV promoter was used (Yuasa *et al.*, 2002). On the other hand, the AAV8 vector transduced antigen-presenting cells (such as dendritic cells) less efficiently than did the rAAV2 vector (Xin *et al.*, 2006). Consequently, gene transduction via the AAV2 vector with the CMV promoter might be less efficient than with rAAV8 and other AAV serotypes.

Because the CMV promoter elicits an immune response against the transgene product (Cordier *et al.*, 2001; Yuasa *et al.*, 2002; Liu *et al.*, 2004), several studies of rAAV-mediated transduction of striated musculature used the muscle creatine kinase (MCK), CK6, or SP6 promoter as a muscle-specific promoter (Gregorevic *et al.*, 2004; Yoshimura *et al.*, 2004; Zhu *et al.*, 2005). Transduction driven by a muscle-specific promoter was achieved without acute toxicological response. Moreover, to enable strong expression in striated muscle, another group created a hybrid promoter containing the MCK enhancer and the simian virus 40 promoter (MCK/SV40 promoter) (Takeshita *et al.*, 2007). The MCK/SV40 promoter yielded long-term (>6 months) expression of a human secretory alkaline phosphatase (huSEAP) reporter gene after electrotransfer of the plasmid into mice. In addition, selection of the rAAV serotype is important. rAAV9 has also been shown to be efficient in cardiac or skeletal muscle transduction (Inagaki *et al.*, 2006; Sarkar *et al.*, 2006).

Our study demonstrated improvement of the contractile force and decreased sensitivity to stretch and exhaustion time for exercise in Sgca$^{-/-}$ muscle after rAAV8-α-SG injection. Recovery of absolute maximal force and specific tetanic force is one of the barometers of amelioration. A dose of about 1×10^{11} VG (for neonates) or 5×10^{11} VG (for adults) in Sgca$^{-/-}$ TA muscle led to transduction of approximately >70% of hind limb muscles and was sufficient to increase the global force of the animal. We compared tetanic contractions of rAAV8-α-SG-injected muscles with those of Sgca$^{+/+}$ and Sgca$^{-/-}$ muscles. The contractile forces of rAAV8-injected Sgca$^{-/-}$ TA and EDL muscles were increased 2-fold compared with that of Sgca$^{-/-}$ muscles. Furthermore, the exercise treadmill test results for rAAV8-injected Sgca$^{-/-}$ mice were higher than those of Sgca$^{-/-}$ mice. This suggested that increased synthesis of α-SG had no adverse effects on SG complex formation, and that overexpression of α-SG might induce stability of the transmembrane without causing muscle pathology. In a therapeutic study using rAAV1 (Fougerousse *et al.*, 2007), injection of rAAV1 encoding α-SG cDNA via the C5-12 promoter (a muscle-specific promoter) into the artery of Sgca$^{-/-}$ mice increased the contractile force of EDL muscles 1.5-fold compared with that of Sgca$^{-/-}$ EDL muscles. Therefore, rAAV8 would be an effective tool for the delivery of therapeutic genes to skeletal muscles in the treatment of limb-girdle muscular dystrophy.

Acknowledgments

The authors greatly appreciate the technical support and helpful discussion provided by Ms. Kazue Kinoshita and Dr. Katsutoshi Yuasa. We thank Dr. Eva Engvall for providing the Sgca$^{-/-}$ mice. This work was supported by a Grant for Research on Nervous and Mental Disorders (16B-2) and by Health Science Research Grants for Research on the Human Genome and Gene Therapy (H16-genome-003) and for Research on Brain Science (H15-kokoro-021 and H18-kokoro-019) from the Ministry of Health, Labor, and Welfare; and by Grants in Aid for Scientific Research (16390418, 16590333, 18590392, and 19390383) from the Ministry of Education, Culture, Sports, Science, and Technology.

References

Akache, B., Grimm, D., Pandey, K., Yant, S.R., Xu, H., and Kay, M.A. (2006). The 37/67-kilodalton laminin receptor is a receptor for adeno-associated virus serotypes 8, 2, 3, and 9. J. Virol. 80, 9831–9836.

Allamand, V., Donahue, K.M., Straub, V., Davisson, R.L., Davidson, B.L., and Campbell, K.P. (2000). Early adenovirus-mediated gene transfer effectively prevents muscular dystrophy in α-sarcoglycan-deficient mice. Gene Ther. 7, 1385–1391.

Araishi, K., Sasaoka, T., Imamura, M., Noguchi, S., Hama, H., Wakabayashi, E., Yoshida, M., Hori, T., and Ozawa, E. (1999). Loss of the sarcoglycan complex and sarcospan leads to muscular dystrophy in β-sarcoglycan-deficient mice. Hum. Mol. Genet. 8, 1589–1598.

Ardini, E., Tagliabue, E., Magnifico, A., Buto, S., Castronovo, V., Colnaghi, M.I., and Menard, S. (1997). Co-regulation and physical association of the 67-kDa monomeric laminin receptor and the $\alpha_6\beta_4$ integrin. J. Biol. Chem. 272, 2342–2345.

Ardini, E., Sporchia, B., Pollegioni, L., Modugno, M., Ghirelli, C., Castiglioni, F., Tagliabue, E., and Menard, S. (2002). Identification of a novel function for 67-kDa laminin receptor: Increase in laminin degradation rate and release of motility fragments. Cancer Res. 62, 1321–1325.

Bonnemann, C.G., Modi, R., Noguchi, S., Mizuno, Y., Yoshida, M., Gussoni, E., McNally, E.M., Duggan, D.J., Angelini, C., and Hoffman, E.P. (1995). β-Sarcoglycan (A3b) mutations cause autosomal recessive muscular dystrophy with loss of the sarcoglycan complex. Nat. Genet. 11, 266–273.

Burton, M., Nakai, H., Colosi, P., Cunningham, J., Mitchell, R., and Couto, L. (1999). Coexpression of factor VIII heavy and light chain adeno-associated viral vectors produces biologically active protein. Proc. Natl. Acad. Sci. U.S.A. 96, 12725–12730.

Cordier, L., Gao, G.P., Hack, A.A., McNally, E.M., Wilson, J.M., Chirmule, N., and Sweeney, H.L. (2001). Muscle-specific promoters may be necessary for adeno-associated virus-mediated gene transfer in the treatment of muscular dystrophies. Hum. Gene Ther. 12, 205–215.

Danieli-Betto, D., Esposito, A., Germinario, E., Sandona, D., Martinello, T., Jakubiec-Puka, A., Biral, D., and Betto, R. (2005). Deficiency of α-sarcoglycan differently affects fast- and slow-twitch skeletal muscles. Am. J. Physiol. Regul. Integr. Comp. Physiol. 289, R1328–R1337.

Dressman, D., Araishi, K., Imamura, M., Sasaoka, T., Liu, L.A., Engvall, E., and Hoffman, E.P. (2002). Delivery of α- and β-sarcoglycan by recombinant adeno-associated virus: Efficient rescue of muscle, but differential toxicity. Hum. Gene Ther. 13, 1631–1646.

Duclos, F., Straub, V., Moore, S.A., Venzke, D.P., Hrstka, R.F., Crosbie, R.H., Durbeej, M., Lebakken, C.S., Ettinger, A.J., Van Der Meulen, J., Holt, K.H., Lim, L.E., Sanes, J.R., Davidson, B.L., Faulkner, J.A., Williamson, R., and Campbell, K.P. (1998). Progressive muscular dystrophy in α-sarcoglycan-deficient mice. J. Cell Biol. 142, 1461–1471.

Ervasti, J.M., Ohlendieck, K., Kahl, S.D., Gaver, M.G., and Campbell, K.P. (1990). Deficiency of a glycoprotein component of the dystrophin complex in dystrophic muscle. Nature 345, 315–319.

Eymard, B., Romero, N.B., Leturcq, F., Piccolo, F., Carrie, A., Jeanpierre, M., Collin, H., Deburgrave, N., Azibi, K., Chaouch, M., Merlini, L., Themar-Noel, C., Penisson, I., Mayer, M., Tanguy, O., Campbell, K.P., Kaplan, J.C., Tome, F.M., and Fardeau, M. (1997). Primary adhalinopathy (α-sarcoglycanopathy): Clinical, pathologic, and genetic correlation in 20 patients with autosomal recessive muscular dystrophy. Neurology 48, 1227–1234.

Fanin, M., Duggan, D.J., Mostacciuolo, M.L., Martinello, F., Freda, M.P., Soraru, G., Trevisan, C.P., Hoffman, E.P., and Angelini, C. (1997). Genetic epidemiology of muscular dystrophies resulting from sarcoglycan gene mutations. J. Med. Genet. 34, 973–977.

Fisher, K.J., Jooss, K., Alston, J., Yang, Y., Haecker, S.E., High, K., Pathak, R., Raper, S.E., and Wilson, J.M. (1997). Recombinant adeno-associated virus for muscle directed gene therapy. Nat. Med. 3, 306–312.

Fougerousse, F., Bartoli, M., Poupiot, J., Arandel, L., Durand, M., Guerchet, N., Gicquel, E., Danos, O., and Richard, I. (2007). Phenotypic correction of α-sarcoglycan deficiency by intra-arterial injection of a muscle-specific serotype 1 rAAV vector. Mol. Ther. 15, 53–61.

Gao, G., Vandenberghe, L.H., Alvira, M.R., Lu, Y., Calcedo, R., Zhou, X., and Wilson, J.M. (2004). Clades of adeno-associated viruses are widely disseminated in human tissues. J. Virol. 78, 6381–6388.

Gao, G.P., Alvira, M.R., Wang, L., Calcedo, R., Johnston, J., and Wilson, J.M. (2002). Novel adeno-associated viruses from rhesus monkeys as vectors for human gene therapy. Proc. Natl. Acad. Sci. U.S.A. 99, 11854–11859.

Greelish, J.P., SU, L.T., Lankford, E.B., Burkman, J.M., Chen, H., Konig, S.K., Mercier, I.M., Desjardins, P.R., Mitchell, M.A., Zheng, X.G., Leferovich, J., Gao, G.P., Balice-Gordon, R.J., Wilson, J.M., and Stedman, H.H. (1999). Stable restoration of the sarcoglycan complex in dystrophic muscle perfused with histamine and a recombinant adeno-associated viral vector. Nat. Med. 5, 439–443.

Gregorevic, P., Blankinship, M.J., Allen, J.M., Crawford, R.W., Meuse, L., Miller, D.G., Russell, D.W., and Chamberlain, J.S. (2004). Systemic delivery of genes to striated muscles using adeno-associated viral vectors. Nat. Med. 10, 828–834.

Imamura, M., Araishi, K., Noguchi, S., and Ozawa, E. (2000). A sarcoglycan–dystroglycan complex anchors Dp116 and utrophin in the peripheral nervous system. Hum. Mol. Genet. 9, 3091–3100.

Imamura, M., Mochizuki, Y., Engvall, E., and Takeda, S. (2005). ε-Sarcoglycan compensates for lack of α-sarcoglycan in a mouse model of limb-girdle muscular dystrophy. Hum. Mol. Genet. 14, 775–783.

Inagaki, K., Fuess, S., Storm, T.A., Gibson, G.A., McTiernan, C.F., Kay, M.A., Nakai, H., Sarkar, R., Mucci, M., Addya, S., Tetreault, R., Bellinger, D.A., Nichols, T.C., and Kazazian, H.H., Jr. (2006). Robust systemic transduction with AAV9 vectors in mice: Efficient global cardiac gene transfer superior to that of AAV8. Mol. Ther. 14, 45–53.

Iwata, Y., Nakamura, H., Mizuno, Y., Yoshida, M., Ozawa, E., and Shigekawa, M. (1993). Defective association of dystrophin with sarcolemmal glycoproteins in the cardiomyopathic hamster heart. FEBS Lett. 329, 227–231.

Janssen, G.M., Kuipers, H., Willems, G.M., Does, R.J., Janssen, M.P., and Geurten, P. (1989). Plasma activity of muscle enzymes: Quantification of skeletal muscle damage and relationship with metabolic variables. Int. J. Sports Med. 10(Suppl. 3), S160–S168.

Kessler, P.D., Podsakoff, G.M., Chen, X., McQuiston, S.A., Colosi, P.C., Matelis, L.A., Kurtzman, G.J., and Byrne, B.J. (1996). Gene delivery to skeletal muscle results in sustained expression and systemic delivery of a therapeutic protein. Proc. Natl. Acad. Sci. U.S.A. 93, 14082–14087.

Kyhse-Andersen, J. (1984). Electroblotting of multiple gels: A simple apparatus without buffer tank for rapid transfer of proteins from polyacrylamide to nitrocellulose. J. Biochem. Biophys. Methods 10, 203–209.

Laemmli, U.K. (1970). Cleavage of structural proteins during the assembly of the head of bacteriophage T4. Nature 227, 680–685.

Li, J., Dressman, D., Tsao, Y.P., Sakamoto, A., Hoffman, E.P., and Xiao, X. (1999). rAAV vector-mediated sarcoglycan gene transfer in a hamster model for limb girdle muscular dystrophy. Gene Ther. 6, 74–82.

Liu, Y.L., Mingozzi, F., Rodriguez-Colon, S.M., Joseph, S., Dobrzynski, E., Suzuki, T., High, K.A., and Herzog, R.W. (2004). Therapeutic levels of factor IX expression using a muscle-specific promoter and adeno-associated virus serotype 1 vector. Hum. Gene Ther. 15, 783–792.

McNally, E.M., Yoshida, M., Mizuno, Y., Ozawa, E., and Kunkel, L.M. (1994). Human adhalin is alternatively spliced and the gene is located on chromosome 17q21. Proc. Natl. Acad. Sci. U.S.A. 91, 9690–9694.

Morgan, J.E., Hoffman, E.P., and Partridge, T.A. (1990). Normal myogenic cells from newborn mice restore normal histology to degenerating muscles of the *mdx* mouse. J. Cell Biol. 111, 2437–2449.

Mourkioti, F., Kratsios, P., Luedde, T., Song, Y.H., Delafontaine, P., Adami, R., Parente, V., Bottinelli, R., Pasparakis, M., and Rosenthal, N. (2006). Targeted ablation of IKK2 improves skeletal muscle strength, maintains mass, and promotes regeneration. J. Clin. Invest. 116, 2945–2954.

Nigro, V., De Sa Moreira, E., Piluso, G., Vainzof, M., Belsito, A., Politano, L., Puca, A.A., Passos-Bueno, M.R., and Zatz, M. (1996). Autosomal recessive limb-girdle muscular dystrophy, LGMD2F, is caused by a mutation in the δ-sarcoglycan gene. Nat. Genet. 14, 195–198.

Noguchi, S., McNally, E.M., Ben Othmane, K., Hagiwara, Y., Mizuno, Y., Yoshida, M., Yamamoto, H., Bonnemann, C.G., Gussoni, E., Denton, P.H., Kyriakides, T., Middleton, L., Hen-

tati, F., Ben Hamida, M., Nonaka, I., Vance, J.M., Kunkel, L.M., and Ozawa, E. (1995). Mutations in the dystrophin-associated protein γ-sarcoglycan in chromosome 13 muscular dystrophy. Science 270, 819–822.

Noguchi, S., Wakabayashi, E., Imamura, M., Yoshida, M., and Ozawa, E. (1999). Developmental expression of sarcoglycan gene products in cultured myocytes. Biochem. Biophys. Res. Commun. 262, 88–93.

Pacak, C.A., Walter, G.A., Gaidosh, G., Bryant, N., Lewis, M.A., Germain, S., Mah, C.S., Campbell, K.P., and Byrne, B.J. (2007). Long-term skeletal muscle protection after gene transfer in a mouse model of LGMD-2D. Mol. Ther. 15, 1775–1781.

Sarkar, R., Mucci, M., Addya, S., Tetreault, R., Bellinger, D.A., Nichols, T.C., and Kazazian, H.H., Jr. (2006). Long-term efficacy of adeno-associated virus serotypes 8 and 9 in hemophilia a dogs and mice. Hum. Gene Ther. 17, 427–439.

Takeshita, F., Takase, K., Tozuka, M., Saha, S., Okuda, K., Ishii, N., and Sasaki, S. (2007). Muscle creatine kinase/SV40 hybrid promoter for muscle-targeted long-term transgene expression. Int. J. Mol. Med. 19, 309–315.

Wang, Z., Zhu, T., Qiao, C., Zhou, L., Wang, B., Zhang, J., Chen, C., Li, J., and Xiao, X. (2005). Adeno-associated virus serotype 8 efficiently delivers genes to muscle and heart. Nat. Biotechnol. 23, 321–328.

Wigler, M., Perucho, M., Kurtz, D., Dana, S., Pellicer, A., Axel, R., and Silverstein, S. (1980). Transformation of mammalian cells with an amplifiable dominant-acting gene. Proc. Natl. Acad. Sci. U.S.A. 77, 3567–3570.

Xiao, X., Li, J., and Samulski, R.J. (1996). Efficient long-term gene transfer into muscle tissue of immunocompetent mice by adeno-associated virus vector. J. Virol. 70, 8098–8108.

Xiao, X., Li, J., and Samulski, R.J. (1998). Production of high-titer recombinant adeno-associated virus vectors in the absence of helper adenovirus. J. Virol. 72, 2224–2232.

Xiao, X., Li, J., Tsao, Y.P., Dressman, D., Hoffman, E.P., and Watchko, J.F. (2000). Full functional rescue of a complete muscle (TA) in dystrophic hamsters by adeno-associated virus vector-directed gene therapy. J. Virol. 74, 1436–1442.

Xin, K.Q., Mizukami, H., Urabe, M., Toda, Y., Shinoda, K., Yoshida, A., Oomura, K., Kojima, Y., Ichino, M., Klinman, D., Ozawa, K., and Okuda, K. (2006). Induction of robust immune responses against human immunodeficiency virus is supported by the inherent tropism of adeno-associated virus type 5 for dendritic cells. J. Virol. 80, 11899–11910.

Yamamoto, H., Mizuno, Y., Hayashi, K., Nonaka, I., Yoshida, M., and Ozawa, E. (1994). Expression of dystrophin-associated protein 35DAG (A4) and 50DAG (A2) is confined to striated muscles. J. Biochem. 115, 162–167.

Yoshida, M., and Ozawa, E. (1990). Glycoprotein complex anchoring dystrophin to sarcolemma. J. Biochem. 108, 748–752.

Yoshimura, M., Sakamoto, M., Ikemoto, M., Mochizuki, Y., Yuasa, K., Miyagoe-Suzuki, Y., and Takeda, S. (2004). AAV vector-mediated microdystrophin expression in a relatively small percentage of *mdx* myofibers improved the *mdx* phenotype. Mol. Ther. 10, 821–828.

Yuasa, K., Sakamoto, M., Miyagoe-Suzuki, Y., Tanouchi, A., Yamamoto, H., Li, J., Chamberlain, J.S., Xiao, X., and Takeda, S. (2002). Adeno-associated virus vector-mediated gene transfer into dystrophin-deficient skeletal muscles evokes enhanced immune response against the transgene product. Gene Ther. 9, 1576–1588.

Zhu, T., Zhou, L., Mori, S., Wang, Z., McTiernan, C.F., Qiao, C., Chen, C., Wang, D.W., Li, J., and Xiao, X. (2005). Sustained whole-body functional rescue in congestive heart failure and muscular dystrophy hamsters by systemic gene transfer. Circulation 112, 2650–2659.

Address reprint requests to:
Dr. Shin'ichi Takeda or Dr. Takashi Okada
Department of Molecular Therapy
National Institute of Neuroscience, NCNP
4-1-1 Ogawa-higashi, Kodaira
Tokyo 187-8502, Japan

E-mail: takeda@ncnp.go.jp or t-okada@ncnp.go.jp

Received for publication January 4, 2008; accepted after revision May 14, 2008.

Published online: June 17, 2008.

THE JOURNAL OF GENE MEDICINE
J Gene Med 2008; **10**: 702–713.
Published online in Wiley InterScience (www.interscience.wiley.com) **DOI:** 10.1002/jgm.1190

RESEARCH ARTICLE

Downstream utrophin enhancer is required for expression of utrophin in skeletal muscle

Jun Tanihata[1,2]
Naoki Suzuki[1,3]
Yuko Miyagoe-Suzuki[1]
Kazuhiko Imaizumi[2]
Shin'ichi Takeda[1]*

[1]*Department of Molecular Therapy, National Institute of Neuroscience, National Center of Neurology and Psychiatry, Ogawa-higashi, Kodaira, Tokyo, Japan*

[2]*Laboratory of Physiological Sciences, Faculty of Human Sciences, Waseda University, Mikajima, Tokorozawa, Japan*

[3]*Department of Neurology, Tohoku University School of Medicine, Seiryo-machi, Sendai, Japan*

*Correspondence to:
Shin'ichi Takeda, Department of Molecular Therapy, National Institute of Neuroscience, National Center of Neurology and Psychiatry, 4-1-1 Ogawa-higashi, Kodaira, Tokyo 187-8502, Japan.
E-mail: takeda@ncnp.go.jp

Received: 17 October 2007
Accepted: 30 January 2008

Abstract

Background Duchenne muscular dystrophy is caused by the absence of the muscle cytoskeletal protein dystrophin. Utrophin is an autosomal homologue of dystrophin, and overexpression of utrophin is expected to compensate for the dystrophin deficit. We previously reported that the 5.4-kb 5′-flanking region of the utrophin gene containing the A-utrophin core promoter did not drive transgene expression in heart and skeletal muscle. To clarify the regulatory mechanism of utrophin expression, we generated a nuclear localization signal-tagged LacZ transgenic (Tg) mouse, in which the LacZ gene was driven by the 129-bp downstream utrophin enhancer (DUE) and the 5.4-kb 5′-flanking region of the utrophin promoter.

Methods Two Tg lines were established. The levels of transgene mRNA expression in several tissues were examined by reverse transcriptase-polymerase chain reaction (RT-PCR) and quantitative RT-PCR. Cryosections of several tissues were stained with haematoxylin and eosin and X-gal.

Results The transgene expression patterns were consistent with endogenous utrophin in several tissues including heart and skeletal muscle. Transgene expression was also up-regulated more in regenerating muscle than in nonregenerating muscle. Moreover, utrophin expression was augmented in the skeletal muscle of DUE Tg/dystrophin-deficient *mdx* mice through cross-breeding experiments. We finally established cultures of primary myogenic cells from this Tg mouse and found that utrophin up-regulation during muscle differentiation depends on the DUE motif.

Conclusions Our results showed that DUE is indispensable for utrophin expression in skeletal muscle and heart, and primary myogenic cells from this Tg mice provide a high through-put screening system for drugs that up-regulate utrophin expression. Copyright © 2008 John Wiley & Sons, Ltd.

Keywords downstream utrophin enhancer; Duchenne muscular dystrophy; dystrophin; transcriptional regulation; transgenic mice; utrophin

Introduction

Duchenne muscular dystrophy (DMD) is an X-linked progressive disorder caused by a defect in the DMD gene, which encodes dystrophin [1]. Dystrophin is a 427-kDa cytoskeletal protein that is normally located on the subsarcolemma and fixed by interaction with dystrophin-associated proteins (DAPs), some of which span the membrane [2–5]. This protein complex links the cytoskeleton of myofibers to the extracellular matrix to

maintain the integrity of the sarcolemma. The lack of dystrophin in DMD causes a secondary loss of DAPs in the sarcolemma and leads to massive muscle necrosis, resulting in cardiomyopathy and early death. Unfortunately, there is no treatment available to stop the progression of this devastating neuromuscular disorder other than corticosteroids. Of the various therapeutic strategies for DMD being developed, up-regulation of utrophin has received considerable attention over recent years.

Utrophin is a 395-kDa cytoskeletal protein with a high degree identity with dystrophin at the amino acid level [6,7] and is an autosomal homologue of dystrophin. It is ubiquitously expressed in most tissues. In embryonic and neonatal skeletal muscles, it is expressed both synaptically and extra-synaptically. In adult skeletal muscle, it is found mostly at the postsynaptic membrane of the neuromuscular junction (NMJ) and the myotendinous junction [8,9].

Mdx mice completely lack the expression of dystrophin, but the signs and symptoms of DMD are not progressive until later in the course of the disease. This mild phenotype can be at least partly explained by up-regulation of utrophin at the sarcolemma [10,11]. Additional studies have shown that utrophin is present in greater amounts in small caliber muscle fibers of *mdx* mice [12,13] and small or regenerating muscle fibers of DMD patients [14,15]. By contrast, utrophin null-*mdx* (dko) mice have a severe myopathic phenotype that is lethal within 20 weeks of birth.

Previous transgenic (Tg) experiments showed that overexpression of utrophin at the sarcolemma compensates for the lack of dystrophin and ameliorates dystrophic phenotypes in dystrophin-deficient *mdx* mice, where components of DAPs had been restored [16–18]. Similarly, adenovirally transduced utrophin ameliorates dystrophic changes in *mdx* mice [19]. We previously reported that the immune response to adenovirally transferred β-galactosidase (β-gal) expression evoked up-regulation of endogenous utrophin, resulting in partial improvement of *mdx* phenotypes [20]. These data suggest that systemic up-regulation of utrophin in DMD patients may lead to an effective treatment for this devastating disorder. However, the regulatory mechanism of utrophin expression is not yet fully understood.

Transcriptional regulation of the utrophin gene is more complicated than previously pictured. Two full-length utrophin mRNAs, A and B, which encode different N-termini, are driven by two distinct promoters [21,22]. Both A- and B-utrophin mRNAs are expressed in a tissue-specific manner, and an immunohistochemical study showed that A-utrophin is expressed in the NMJ, choroid plexus, pia mater, and renal glomerulus and tubule [11]. On the other hand, B-utrophin is expressed in vascular endothelial cells [11]. Several short C-terminal utrophin isoforms have been also reported, as found in dystrophin [23]. To elucidate the transcriptional regulation of the utrophin gene, a more powerful tool is engineering an *in vivo* mouse model carrying a reporter gene. We previously generated a transgenic mouse (Gnls) in which the LacZ gene was driven by the 5385-bp 5′-flanking region containing the A-utrophin promoter [24]. Expression of β-gal protein and mRNA derived from the transgene coincided well with the endogenous expression of utrophin in liver, testis, colon, submandibular gland, and small intestine, but β-gal expression was extremely low in skeletal and cardiac muscle. These results suggested that muscle repressor elements may be present in the 5385-bp region or that another regulatory element outside the region might be required for the expression in striated muscle. Comparable results were found by Weir *et al.* [25] by using a transgene covering 3.8 kb of the mouse promoter region, which included the 1.3-kb reporter sequence characterized by Dennis *et al.* [21].

Recently, the downstream utrophin enhancer (DUE) region was identified and located approximately 9 kb downstream of the second intron. The upstream utrophin promoter is under the control of DUE [10,26]. Therefore, in the present study, we generated transgenic mice (DUE Tg) in which DUE was added upstream of the 5385-bp 5′-flanking region and analysed the expression pattern of the transgene in several tissues. We found that the LacZ genes were expressed in skeletal and cardiac muscles. These data are very relevant to finding a way to up-regulate utrophin expression, and DUE mice as well as the primary cells derived from the mice are available for that purpose.

Materials and methods

Construction of transgene and generation of transgenic mice

To further investigate the utrophin A promoter activity in our previous report, genomic fragments containing the 5′ end of the mouse A-utrophin gene were cloned from a 129Sv mouse genomic library (Stratagene, Inc., La Jolla, CA, USA). One clone contained the 5385-bp 5′-flanking region of the A-utrophin gene, the complete exon 1A, and the first 59 bp of the exon 2 untranslated region (UTR). The genomic fragment was fused in-frame to an nls (from SV40T antigen)-tagged LacZ gene [27] (pCMVb; Clontech, San Jose, CA, USA), followed by a rabbit β-globin polyA signal in Bluescript II (Stratagene) [24]. Furthermore, we inserted the 129-bp utrophin enhancer region that is found in utrophin gene intron 2 [26] upstream of this fragment (Figure 1A). The DNA fragment containing the transgene expression cassette was purified from agarose gel and injected into fertilized C57BL/6J eggs by YS Institute (Utsunomiya, Tochigi, Japan) (Figure 1B). We obtained two transgenic F0 (downstream utrophin enhancer/A promoter-nls LacZ transgenic mice), and two transgenic lines were established by mating the founders with C57BL/6J mice (B6) (Figure 1C). To obtain transgenic *mdx* (Tg/*mdx*) male mice, we mated Tg male mice with *mdx* female mice (Figure 1D).

J Gene Med 2008; **10**: 702–713.
DOI: 10.1002/jgm

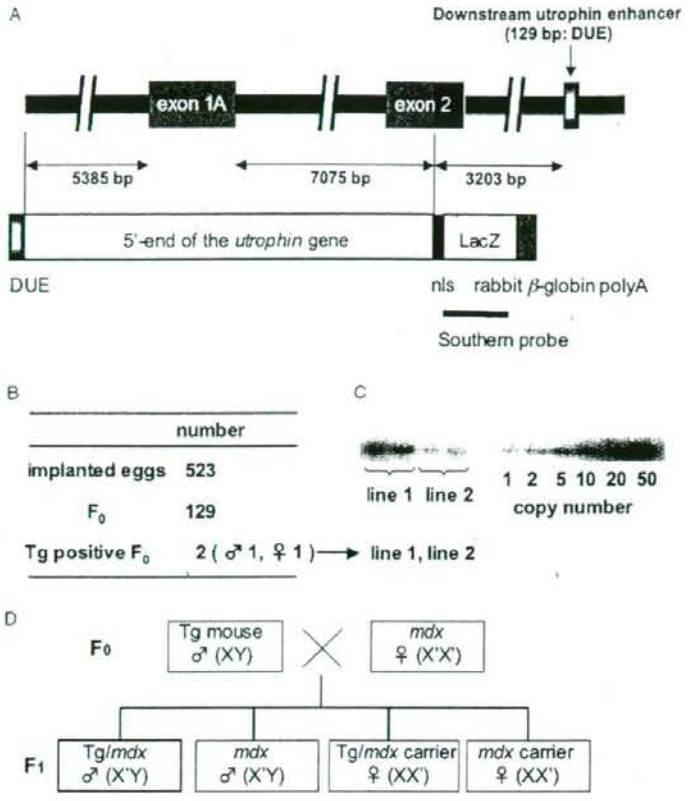

Figure 1. Generation of downstream utrophin enhancer/A-utrophin promoter-nls LacZ Tg mice. (A) Diagram of the transgene used in this study. The genomic fragment (12.9 kb), which contained the 129-bp DUE, 5385-bp 5'-flanking region of the A-utrophin gene, exon 1A, intron 1, and the first 59 bp of exon 2 UTR, was fused in-frame to the nls-tagged LacZ gene. The black bar indicates the Southern probe used to determine genotypes. (B) Summary of generation of Tg mice. (C) Determination of copy numbers in Tg mice by Southern blotting (left). The vector plasmids containing the transgene served as a standard to estimate the number of copies of the transgene (right). (D) Generation of Tg/mdx mice. The bold box indicates the Tg/mdx male mice used in the present study

Animals

C57BL/6J and *mdx* mice aged 5–12 weeks, Tg mice and their wild littermates aged 3–18 weeks, and Tg/*mdx* mice aged 3–7 weeks were used. All animals were housed in a separate room at a temperature of 20–22 °C and under a 12:12 h light/dark cycle. Animals were sacrificed by cervical dislocation. All protocols were approved by the Institutional Animal Care and Use Committee of the National Institute of Neuroscience and were performed in compliance with the 'Guide for the Care and Use of Animals' of the Division of Laboratory Animal Resources.

Genotyping

Tg mice were screened by Southern blotting of genomic DNA from their tails. Genomic DNA was isolated using a lysis buffer [50 mM Tris-HCl, pH 8.0, 0.1 M NaCl, 20 mM ethylenediaminetetraacetic acid, 1% sodium dodecyl sulfate (SDS)] with proteinase K (0.15 mg/ml) and pronase E (1 mg/ml) digestion. Genomic DNA (10 μg) was digested by *BamH*I, separated on a 0.8% agarose gel, and transferred to Hybond-N+ membranes (Amersham Biosciences, Bucks, UK). A 3072-bp DNA fragment of the LacZ gene was labelled with ^{32}P-dCTP as a Southern probe, and hybridized with membranes at 65 °C overnight. The membranes were then washed extensively [2 × saline sodium phosphate-EDTA (SSPE), 0.1% SDS; 1 × SSPE, 0.1% SDS; 0.1 × SSPE, 0.1% SDS] at 65 °C and analysed by BAS 2500 (Fuji Film, Tokyo, Japan).

Isolation of total RNA from mice and myogenic cells

Three- to 8-week-old Tg mice and their wild-type littermates were sacrificed, and tissues were isolated and rapidly frozen in liquid nitrogen. Total RNA was isolated from frozen tissues and myogenic cells using TRIzol reagent (Invitrogen Life Technologies, Carlsbad, CA, USA) according to the manufacturer's protocol.

Reverse transcription-polymerase chain reaction (RT-PCR) and quantitative real-time PCR (q-RT-PCR)

RT was performed with 1.0 μg of total RNA using a QuantiTect Reverse Transcription Kit (Qiagen, Valencia, CA, USA) according to the manufacturer's protocol. PCR was performed using LacZ sense (5′-CGACATTGGCGTAAGTGAAG-3′) and antisense (5′-ATCGCCATTTGACCACTACC-3′) primers for 30 cycles (denaturation at 95 °C for 1 min, annealing at 60 °C for 30 s, and extension at 72 °C for 1 min). As a control for the generation of PCR products due to residual contamination of genomic DNA, an equivalent amount of RNA that had not been treated with RT was also processed in parallel. The RT-PCR products of all samples were compared with the levels of a housekeeping gene, 18 s rRNA, amplified with the following primer pair: sense (5′-TACCCTGGCGGTGGGATTAAC-3′) and anti-sense (5′-CGAGAGAAGACCACGCCAAC-3′) primers. The levels of various cDNAs were determined by q-RT-PCR using SYBR Green from ABI PRISM 7700 (Applied Biosystems, Foster City, CA, USA). Each result shows the average of three or four samples. The LacZ and 18 s rRNA primer sequences are described above. A-utrophin: sense (5′-ATGGCCAAGTATGGGGACCTTG-3′) and anti-sense (5′-GTGGTGAAGTTGAGGACGTTGAC-3′) primers; myogenin: sense (5′-CATGGTGCCCAGTGAATGCAACTC-3′) and anti-sense (5′-TATCCTCCACCGTGATGCTGTCCA-3′) primers; and MEF2C: sense (5′-TGGACAACAAAGCCCTC-AGCAGGT-3′) and anti-sense (5′-AATCCCTGCTTCGTTC-CCTCTGC-3′) primers were designed for q-RT-PCR. 18 s rRNA mRNA was amplified as an internal control.

Histochemical analysis

After Tg and wild-type mice were sacrificed, the cerebrum, cerebellum, submandibular gland, lung, liver, kidney, small intestine, colon, testis, tibialis anterior (TA) and gastrocnemius (GC) muscles, diaphragm, and heart were isolated and frozen in liquid nitrogen-cooled isopentane. Cryosections (7 μm) from several tissues were stained with haematoxylin and eosin (H&E) and with 5-bromo-4-chloro-3-indolyl-β-D-galactopyranoside (X-gal; Wako Chemicals, Osaka, Japan) as described previously [28]

Immunohistochemistry

Serial transverse cryosections (7 μm) from different tissues were placed on slides, then dried and fixed in acetone for 10 min at −20 °C. We carried out immunohistochemical analysis with a rabbit polyclonal antibody against human utrophin (UT-2) that recognizes amino acid positions 1768–2078 [29]. The primary antibodies were detected with Alexa 488-labelled goat anti-rabbit IgG (Molecular Probes, Eugene, OR, USA). The nucleus was stained with TOTO-3 iodide (Molecular Probes). The NMJ was stained with Alexa 594-labelled α-bungarotoxin (α-BTX) (Molecular Probes). Signals were recorded photographically with a laser-scanning confocal imaging system (TCSSP; Leica Microsystems, Wetzlar, Germany).

Cardiotoxin injection

To cause muscle degeneration, we injected 100 μl of cardiotoxin (CTX) of *Naja naja atra* venom (10 μM in saline; Wako Chemicals) into the right TA and GC muscles of 5- to 7-week-old Tg mice using a 29-gauge needle. The concentration of CTX was determined as described previously [30]. CTX-injected Tg mice were sacrificed 1–14 days after injection. The CTX-injected and contralateral non-injected TA and GC muscles were isolated and frozen in liquid nitrogen-cooled isopentane. Cryosections (7 μm) were stained with H&E and X-gal. At the same time, serial cryosections (7 μm) were stained with UT-2 together with Alexa 594-labelled α-BTX. Total RNA was isolated from these frozen tissues.

Cell preparation and culture

Mouse-derived mononucleated cells were prepared from DUE and Gnls Tg mice and C57BL/6J mice as previously described [31]. Primary myoblasts were cultured alone with growth medium (GM): F-10 containing 20% fetal bovine serum, 1% penicillin-streptomycin (Invitrogen), and 2.5 ng/ml basic fibroblast growth factor (Invitrogen) in collagen-coated dishes (Iwaki, Tokyo, Japan) or chamber slides (Nalge Nunc, Rochester, NY, USA) coated with collagen type I (Upstate, Waltham, MA, USA). For differentiation, the medium was changed to a differentiation medium (DM; 5% horse serum in Dulbecco's modified Eagle's medium) and cultured 5 days. GM and DM were replenished every 24 h [32].

Statistical analysis

Statistical differences were determined by Student's unpaired *t*-test. All data are expressed as means ± SE. $p < 0.05$ was considered statistically significant.

Results

Generation of downstream utrophin enhancer/A promoter-nls LacZ transgenic (DUE Tg) mice

Two F0 'founder' mice were identified by Southern blotting analysis using a LacZ cDNA probe, and two transgenic lines were established (Figure 1B). The approximate numbers of transgene copies were

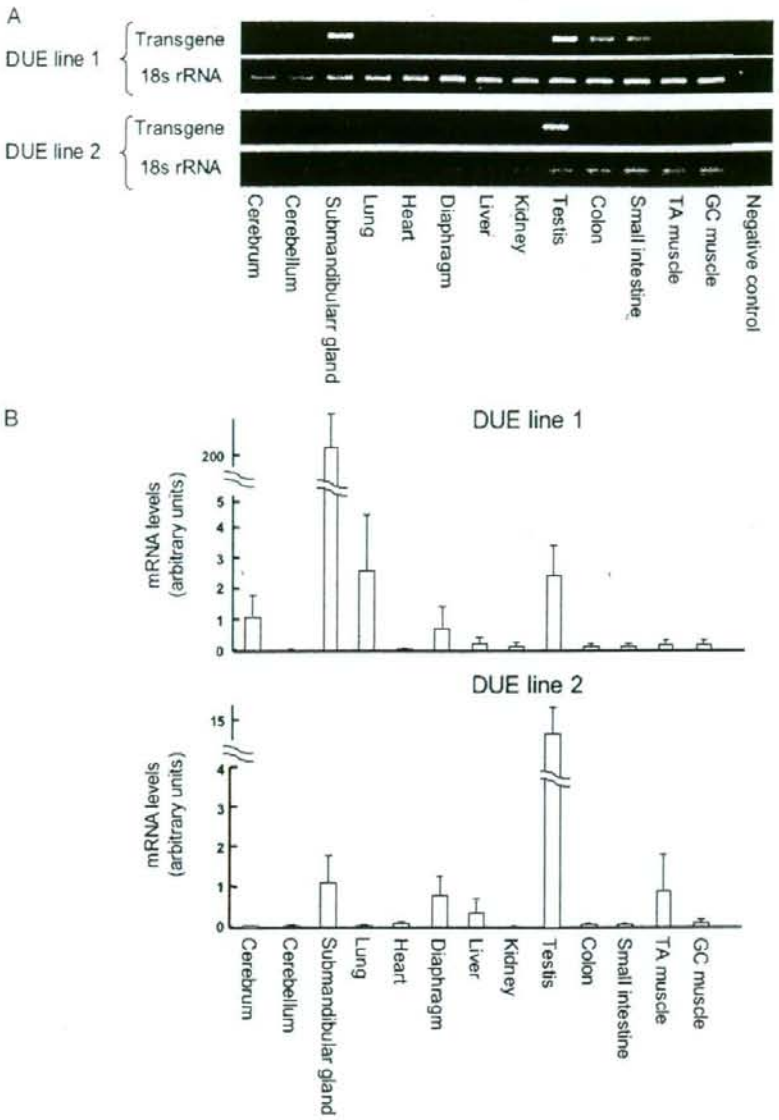

Figure 2. Transgene mRNA expression in several tissues of Tg mice. (A) Representative photomicrographs of EtBr-stained agarose gels depicting cDNA products of the transgene and 18s rRNA from RT-PCR analysis of total RNA from several tissues in Tg mice. (B) Quantification of q-RT-PCR products of the transgene were done by optimization to expression of 18s rRNA in several tissues. The ratio of the transgene to 18s rRNA is shown as the mean ± SEM of four independent experiments performed in triplicate

approximately 15 in line 1 or approximately two in line 2 (Figure 1C).

The levels of transgene expression in several tissues were determined by RT-PCR and q-RT-PCR (Figures 2A and 2B). High levels of transgene mRNA expression were detected in the submandibular gland, testis, lung, colon, and small intestine of DUE line 1 Tg mice and in the submandibular gland and testis of DUE line 2 Tg mice. The signals were weakly detected in other tissues of DUE line 2 Tg mice, probably because there were fewer copies of the transgene.

Comparison of β-gal and endogenous utrophin expression in DUE Tg mice

To compare β-gal expression derived from the transgene with endogenous utrophin expression, cryosections were stained with X-Gal, and then serial cryosections were stained with either H&E or UT-2, a polyclonal antibody against human utrophin [29] (Figure 3). UT-2 recognized only the full-length A- and B-utrophin [29]. We found that β-gal expression coincided well with endogenous utrophin expression in the liver, testis, colon, submandibular gland, small intestine, kidney, and lung (Figure 3A). When

J Gene Med 2008; **10**: 702–713.
DOI: 10.1002/jgm

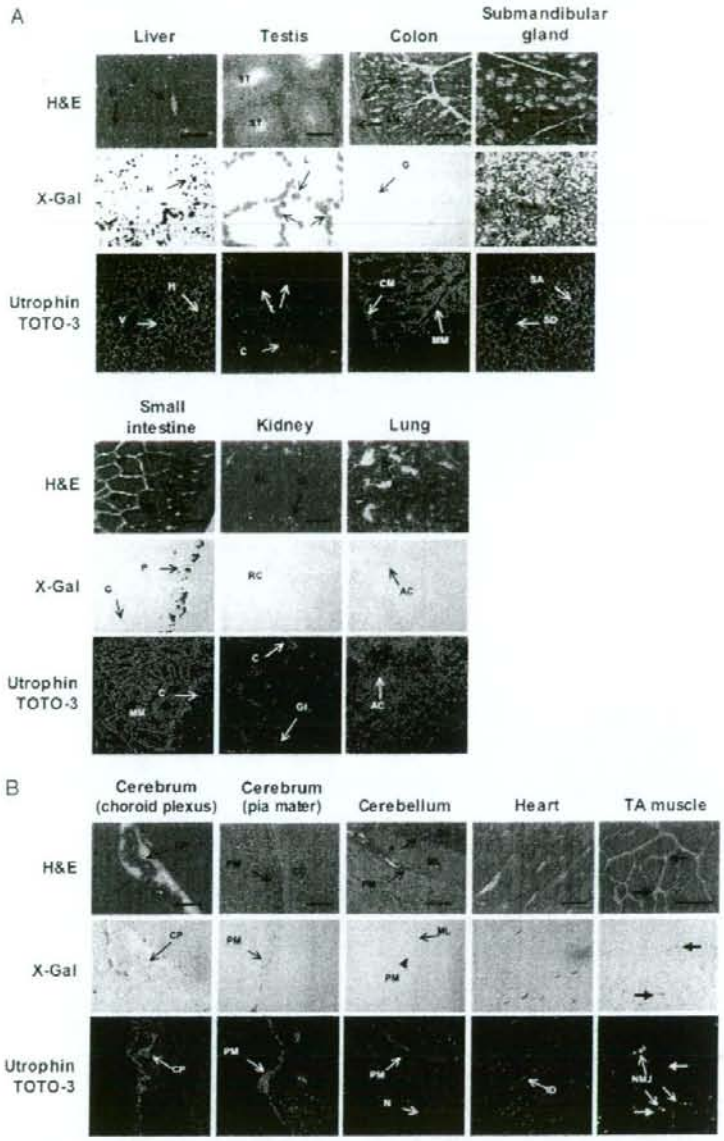

Figure 3. Histological and immunohistochemical analysis of DUE Tg mice. Serial cryosections of tissues [liver, testis, colon, submandibular gland, small intestine, kidney, and lung (A), cerebrum, cerebellum, heart, and TA muscle (B)] from 7-week-old DUE line 1 Tg mice were stained with H&E (top), X-Gal (middle), and a polyclonal antibody against utophin (UT-2; green) (bottom). Nuclei were stained with TOTO-3 (blue). The NMJs were identified with α-BTX (red) in TA muscle. V, terminal hepatic venule; Si, sinusoid; H, hepatocyte; ST, seminiferous tubule; L, Leydig cell; S, Sertoli cell; C, capillary; CM, inner circular muscle layer; G, goblet cell; LM, outer longitudinal muscle layer; MM, muscularis mucosa; SD, striated duct; Sc, serous secretory cell; SA, serous acinus; Vi, villus; Cr, crypt; P, Paneth cell; C, capillary; RC, renal cortex; Gl, glomerulus; AC, alveolar cells; CP, choroid plexus; PM, pia mater; CC, cerebral cortex; N, neuron; ML, molecular layer; GL, granular layer; P, Purkinje cell; ID, intercalated disk; NMJ, neuromuscular junction. Scale bar = 100 μm

compared with β-gal expression in Gnls Tg mice, the expression levels of the transgene in DUE Tg mice were similar in the liver, testis, colon, submandibular gland, and small intestine, but were elevated in the kidney and lung. In addition, when transgene expression was examined at the protein level, the levels were higher in DUE line 1 Tg mice than those in line 2 Tg mice.

In the liver, the nuclei of hepatocytes, but not sinusoid lining cells, were strongly stained with X-gal, whereas endogenous utrophin was detected in the margins of hepatocytes along sinusoids and terminal hepatic venules.

In the testis, β-gal activity was found in Sertoli cells in the basal compartment of the seminiferous tubules, but not in the adluminal compartment, and in Leydig

J Gene Med 2008; 10: 702–713.
DOI: 10.1002/jgm

cells in the interstitial supporting tissues between the seminiferous tubules. Consistent with this observation, endogenous utrophin signals were found along the basement membrane of the seminiferous tubules and Leydig cells.

In the colon, β-gal-positive nuclei were found in goblet cells in large intestinal glands. Endogenous utrophin signals were found along the basement membrane of large intestinal glands and the muscularis mucosa.

In the submandibular gland, the nuclei of both serous and mucous secretory cells were clearly stained with X-gal. The striated duct epithelia lacked the β-gal signal. Endogenous utrophin was detected along the basement membrane of serous and mucous acini, but not of striated ducts.

In the small intestine, β-gal-positive nuclei were found in goblet cells and Paneth cells, which lie in epithelia of the bases of villi and crypts. Endogenous utrophin signals were found along the basement membrane of villi and crypts and in the muscularis mucosa.

In the kidney, β-gal-positive nuclei were found in the epithelia of cortical renal tubules, but not in glomeruli. It is not clear whether β-gal positive nuclei were present in proximal convoluted tubules, distal convoluted tubules, collecting tubules, or collecting ducts, although endogenous utrophin was found along the basement membrane of cortical renal tubules, collecting ducts of the renal medulla and Bowman's capsules, and in glomerular capillaries.

In the lung, β-gal-positive nuclei were found in alveoli, but not in terminal bronchiole epithelia. It is not clear whether β-gal-positive nuclei were present in type I or type II pneumocytes. Endogenous utrophin was found in alveolar cells and terminal bronchiole epithelia. In these tissues, endogenous utrophin seemed to localize at the plasma membranes of cells adjacent to the basement membranes.

β-gal expression in cerebrum, cerebellum, heart, and skeletal muscle of DUE Tg mice

In a previous study of Gnls Tg mice, we did not detect any β-gal expression in the cerebrum, cerebellum, heart, and skeletal muscle [24], but we found β-gal expression in these tissues in the DUE line 1 Tg mice (Figure 3B).

In the cerebrum, β-gal positive nuclei were found in ependymal cells of the choroid plexus and in fibroblastic cells of the pia mater along the basal membrane. Consistent with this observation, endogenous utrophin was detected in the choroid plexus and pia mater.

In the cerebellum, β-gal-positive nuclei were found in stellate and basket cells of the molecular layer, but not in fibroblastic cells of the pia mater, although endogenous utrophin is expressed in the pia mater of the cerebellum. Our results indicate that the distal utrophin enhancer cannot activate expression of the transgene in fibroblastic cells of the pia mater in the cerebellum, although it can enhance the expression in fibroblastic cells of the pia mater in the cerebrum.

In the heart, β-gal is expressed in myocardial nuclei located in the vicinity of intercalated disks. Endogenous utrophin expression was found in intercalated disks and T tubules of cardiac muscle.

In skeletal muscle, A-utrophin is expressed in NMJs, peripheral nerves, and larger blood vessels. We detected β-gal expression not only in myonuclei located close to NMJs, but also in myonuclei remote from NMJs in DUE Tg skeletal muscles, although it is not clear whether β-gal-positive nuclei were present in nerves and blood vessels. Expression of the transgene was not detected in the cerebrum, cerebellum, heart, and skeletal muscle in DUE line 2 Tg mice.

β-gal expression was augmented in CTX-injected and dystrophin-deficient DUE Tg mice

We examined expression of the transgene under a condition in which expression of endogenous utrophin is augmented. Recently, Galvagni *et al.* [10] reported that the transcription of A-utrophin was activated in regenerating muscle under DUE control. Therefore, we injected CTX into TA muscles of Tg mice to damage muscle fibers, and analysed β-gal expression during muscle regeneration (Figure 4). The β-gal signals were strongly detected in extrasynaptic regions at 5 or 7 days after CTX injection (Figure 4A). Moreover, transgene mRNA levels were also elevated at 3 or 5 days after CTX injection (Figure 4B). These transgene expressions coincided well with the expression of endogenous utrophin. It is interesting to note that transgene expression was also augmented in CTX-injected DUE line 2 Tg mice, although transgene expression was not detected in non-injected skeletal muscle of these mice (Figure 4C).

Utrophin was also up-regulated in the dystrophic process of *mdx* mouse skeletal muscle. To examine the transgene expression in dystrophin-deficient muscle, we mated DUE line 2 Tg male mice with *mdx* female mice (Figure 1D). Endogenous utrophin was overexpressed along the sarcolemma, and some myonuclei of TA and GC muscles of DUE line 2 Tg/*mdx* male mice were positive for β-gal (Figure 5A). We also found slightly elevated mRNA levels derived from the transgene in TA and GC muscles of DUE line 2 Tg/*mdx* mice by RT-PCR (Figure 5B).

Transgene expression was activated in late stage muscle differentiation *in vitro*

We cultured primary myoblasts from skeletal muscles of DUE Tg and Gnls Tg mice, and some of the cultures were induced to differentiate. Those cells were stained with X-Gal (Figure 6A). Expression of the transgene was detected in primary myoblasts of DUE Tg mice, but

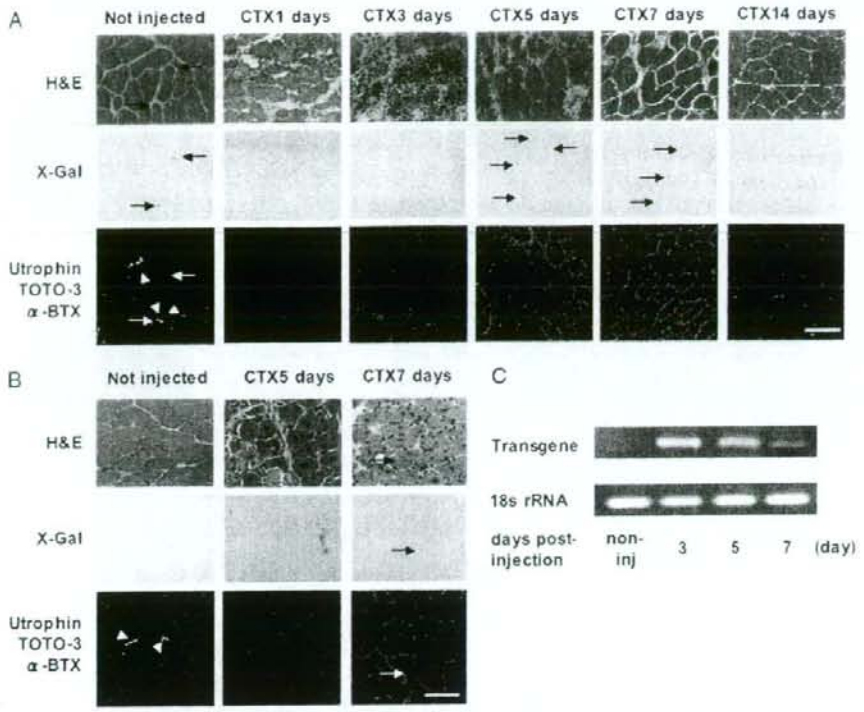

Figure 4. Transgene expression during muscle regeneration in CTX-injected DUE Tg mice. Cryosections of muscles were stained with H&E (top), X-Gal (middle), and a polyclonal antibody against utophin (UT-2; green) (bottom). Nuclei were stained with TOTO-3 (blue). The NMJs were identified with α-BTX (red). (A) TA muscle of DUE line 1 Tg mice at 0, 1, 3, 5, 7, or 14 days after CTX injection. (B) TA muscle of DUE line 2 Tg mice at 0, 5, or 7 days after CTX injection. Arrowhead, NMJ; scale bar = 100 μm. (C) Representative photomicrographs of EtBr-stained agarose gels depicting cDNA products for the transgene and 18s rRNAs from RT-PCR analysis of total RNA from CTX-injected TA muscle of DUE line 1 Tg mice at 0, 3, 5, or 7 days after CTX injection

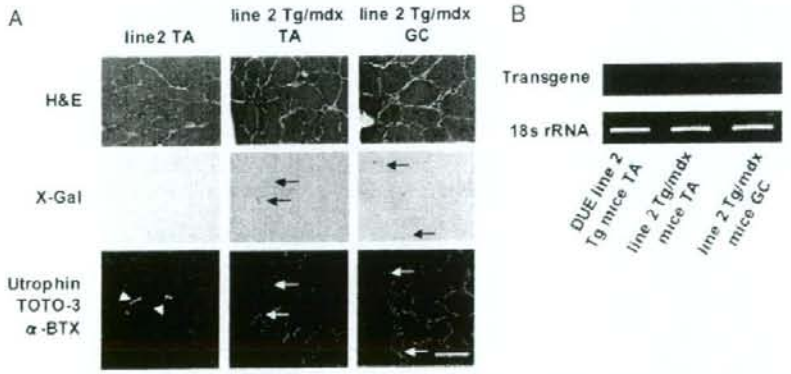

Figure 5. Transgene expression in skeletal muscle of DUE Tg mice cross-bred with dystrophin-deficient mdx mice. (A) Cryosections of muscles were stained with H&E (top), X-Gal (middle), and a polyclonal antibody against utophin (UT-2; green) (bottom). Nuclei were stained with TOTO-3 (blue). The NMJs were identified with α-BTX (red). TA and GC muscles of DUE line 2 Tg/mdx mice. Arrow, β-gal-expressing nuclei; scale bar = 100 μm. (B) Representative photomicrographs of EtBr-stained agarose gels depicting cDNA products for the transgene and 18s rRNAs from RT-PCR analysis of total RNA from TA and GC muscles of DUE line 2 Tg/mdx mice. As a control, the TA muscle of DUE line 2 Tg mice was used

not in those of Gnls Tg mice (Figure 6). In addition, the expression was up-regulated in myotubes in the DUE Tg mice, but not altered in myotubes of the Gnls Tg mice (Figures 6B and 6C). The up-regulation of the transgene was further investigated at the mRNA level, and it was found at a later stage of muscle differentiation. Interestingly, the expression profiles of β-gal and endogenous utrophin were in accordance with that of MEF2C, but not compatible with that of myogenin.

J Gene Med 2008; 10: 702–713.
DOI: 10.1002/jgm

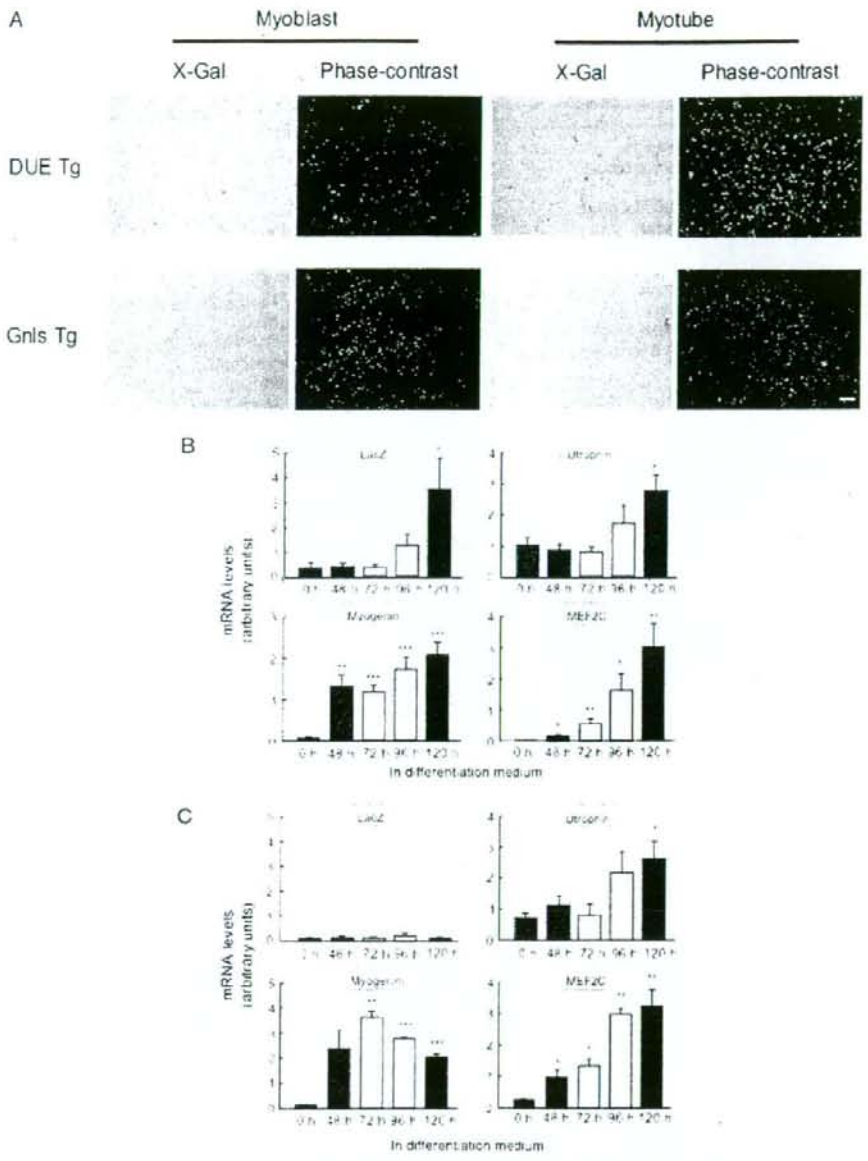

Figure 6. Transgene expression in primary cultured myoblasts and myotubes from DUE Tg mice. (A) Primary cultured myoblasts and myotubes from DUE Tg mice and Gnls Tg mice were stained with X-Gal. Image of myotube after 3 days in differentiation medium. Scale bar = 200 μm. (B, C) Quantification of q-RT-PCR products for transgene, A-utrophin, myogenin, and MEF2C optimized to expression of 18s rRNA in primary myoblasts and myotubes from DUE Tg mice and Gnls Tg mice. The ratios of the transgene, A-utrophin, myogenin, and MEF2C to 18s rRNA are shown as the mean ± SEM of four independent experiments performed in triplicate. *$p < 0.05$, **$p < 0.01$ and ***$p < 0.001$ (versus 0 time)

Discussion

We previously showed that a 5385-bp 5′-flanking region of the utrophin gene containing the A-utrophin core promoter drives high levels of transgene expression in liver, testis, colon, submandibular gland, and small intestine, but not in heart and skeletal muscle [24]. In the present study, we demonstrated that addition of DUE to the 5385-bp 5′-flanking region enabled transgene expression in a pattern that was almost identical to that endogenous utrophin expression (Tables 1 and 2). Moreover, β-gal-expressing nuclei were basically located in the vicinity of the endogenous utrophin expression in heart and skeletal muscle.

In regenerating muscle of DUE Tg mice and skeletal muscle of DUE Tg/*mdx* mice, which lack dystrophin, the transgene expression was considerably